Islamic University of Gaza
Deanery of Graduate studies
Faculty of Science
Physics Department

METAMATERIAL OPTICAL WAVEGUIDE SENSORS

By
Emad M. A. Mehjez

Supervised By
Prof. Dr. Mohammed M. Shabat,
and
Dr. Hala J. Khozondar

"A Thesis Submitted in Partial Fulfillment of the Requirements for the Degree of Master of Science in Physics"

2008 - 1429

Abstract

Propagation of electromagnetic waves in linear and nonlinear media has received an increasing attention from researchers in the optoelectronics field.

A great attention is nowadays paid to optical waveguide sensors because they offer many advantages such as: small size, low price, safe when used in aggressive environments and mechanically stable.

Many theoretical studies concerning analysis of dispersion equations were introduced for many planar waveguide structures, and some authors have proposed scaling rules and universal dispersion analysis.

Homogeneous sensors are mainly used in concentration measurements while surface sensors are used in detecting of adsorbed layers .

The type of waveguides mostly used in chemical and medical sensing is the planner optical waveguide structure with normal asymmetry (i.e. the substrate refractive index being greater than that of the cover).

Sensitivity of measuring the physical or chemical quantities appearing in the cover region depends on the strength and distribution of the evanescent field in that cover. Sensitivity optimization requires suitable choice of the guiding layer thickness and the materials from which sensor layers are constructed, so that the sensor may exhibit its maximum sensitivity .

Scientists have proposed various types of these sensors and theoretically analysed them and suggested solutions for constructing highly efficient sensors.

In this thesis, we investigate nonlinear waveguide sensors when the guiding layer is a Left- Handed material (LHM) for both transverse electric (TE) and transverse magnetic (TM) waves. We consider the case when the analyte homogenously distributed in the cladding, i.e., homogenous sensing. The proposed structure consists of a left-Handed material (LHM) as a guiding layer sandwiched between a linear substrate and a nonlinear cover with an intensity dependent refractive index.

The dispersion relation of the proposed structure is derived and the sensitivity of the effective refractive index to variations in the refractive index of the cladding is obtained. The condition required for the sensor to exhibit its maximum sensitivity is presented. The variation of the sensitivity with different parameters of the structure is studied and explained. The power flow through the sensor layers is also considered because the fraction of total power flowing in the covering medium is related to sensitivity.

With respect to planar optical waveguide sensors, the main remarks gained from our investigations can be summarized as follows:

• There is a close connection between the fraction of total power propagating in the covering medium and the sensitivity of the sensor. In most cases, they may be regarded as nearly identical thus the enhancement of the fraction of total power flowing in the cladding is essential for sensing applications.

• As the nonlinearity of the cladding increases, the wave crest is displaced towards the cladding and as a result the sensitivity of the optical waveguide sensor is enhanced.

• Cladding to film permittivity ratio should be as high as possible but substrate to film permittivity ratio should be as low as possible to increase the evanescent field tail in the cladding and to reduce it as possible in the substrate. The inversion of the conventional waveguide symmetry is strongly recommended if possible. In some cases it is not possible especially when the analyte is air.

ملخص البحث

تحظى مسألة انتشار الموجات الكهرومغناطيسية في الأوساط المختلفة الخطية منها و اللاخطية باهتمام متزايد من قبل الباحثين في حقل الالكترونيات البصرية في الآونة الأخيرة ، ولقد عمد الكثير منهم إلى حل معادلات ماكسويل في عدة طبقات ، واقترح آخرون صيغ عامة يمكن تطبيقها على نبائط مؤلفة من عدة طبقات (multi-layer planner waveguides).

إن من أهم استخدامات المسالك الموجية (optical waveguides) أنها أساس في صناعة المجسات الضوئية وبخاصة في أبحاث الاستشعار الكيميائي الحيوي بحيث يتم تحويل التغيرات المصاحبة لتفاعل كيميائي أو حيوي أو الناتجة عن ترسيب طبقات معينة (بروتين – بكتيريا – مضادات حيوية ...) إلى نبضة يمكن قياسها اعتمادا على التغيرات الحاصلة في الصفات الضوئية في طبقات المجس.

يتمتع هذا النوع من المجسات بأهمية خاصة بسبب ما تتميز به من صغر حجمها و رخص ثمنها وثباتها الكيميائي والميكانيكي عادة وإمكانية استخدامها في المناطق الخطرة دون خطر الانفجار ونحوه .

وبناء على ما تقدم ، اقترح العلماء نماذج عديدة لهذه المجسات وقاموا بتحليلها نظريا وقدموا حلولا لبناء مجسات ذات كفاءة عالية ، إلا أن غالبية هذه الأبحاث ركزت على النوع الخطي فقط ، ولم تتعرض باستفاضة إلى المجسات اللاخطية .

لقد تم في هذه الأطروحة دراسة المجسات اللاخطية وذلك عندما يكون المسلك الأساسي (guiding film) من مواد يسارية (LHMs) في كل من المسالك الموجية ذات الطابع الكهربي المستعرض والمغناطيسي المستعرض على حد سواء
(transverse electric and transverse magnetic waves)، وتركزت الدراسة على الاستشعار المتجانس (homogeneous sensing).

المجس المقترح يتعامل مع ثلاثة أوساط على شكل شرائح مختلفة وهي عبارة عن طبقة وسطى من مواد يسارية (LHMs) محاطة من أعلى بوسط غير خطي ومن أسفل بوسط خطي.

لقد تم تطبيق معادلات ماكسويل في الطبقات المختلفة للمجس وعرض الحلول المناسبة لها ثم طبقت الشروط الحدية والتي من خلالها تم الحصول على معادلة التشتت للنظام قيد الدراسة والتي أمكن من خلالها تقديم شكل رياضي يحكم حساسية المجس .

هذه الحساسية بدورها أخضعت لمعالجات رياضية للحصول على الشرط اللازم لكي تكون حساسية المجس أكبر ما يمكن ، وتم تقديم نموذج نظري لهذا المجس حدد فيه سمك الطبقة الوسطى (wave guiding film width) الذي يجعل استجابة المجس أكبر ما يمكن .

وتم كذلك دراسة تدفق الطاقة (power flow) عبر طبقات المجس وذلك من أجل تفسير ما عرض لنا من نتائج وتأكيد وجود تلك النهاية العظمى في تصرف الحساسية مع تغير سمك الطبقة الوسطى .

تبين من الدراسة أن ثمة صلة وثيقة بين الجزء الضئيل من إجمالي الطاقة التي تتدفق في الطبقة العلوية وحساسية أجهزة الاستشعار وفي معظم الحالات يمكن اعتبارها متطابقة تقريبا وبالتالي فإن تعزيز نسبة إجمالي الطاقة المتدفقة في الطبقة العلوية أمر أساسي لتطبيقات الاستشعار .

كلما زادت اللاخطية في الطبقة العلوية انزاحت قمة الموجة نحو الطبقة العلوية وبالتالي ازدادت حساسية المجس .

نسبة سماحية الطبقة العليا إلى الطبقة الوسطى يجب ان تكون عالية ما امكن بينما نسبة سماحية الطبقة السفلية الى الطبقة الوسطى يجب ان تكون في الحد الأدنى لزيادة نسبة المجال المضمحل في الطبقة العلوية وتقليله ما أمكن في الطبقة السفلية، لذلك فإن المجس الضوئي معكوس التماثل ($n_c \succ n_s$) يوصى به بشدة في الحالات التي يمكن فيها الحصول على هذا التماثل المعكوس.

Dedication

To the soul of my father…

To my loving and caring mother…

To my aunt whose continuous assistance

and encouragement was of great help…

To my devoted wife…

To my children…

I dedicate this thesis.

***

Acknowledgments

I would like to acknowledge my indebtedness and gratefulness to my supervisors Prof. Dr. M. M. Shabat and Dr. Hala J. Khozondar whose without their guidance, encouragement , and advice this thesis wouldn't have been completed successfully.

A special word of thank is due to Dr. Sofyan Taya Who guided me throughout this thesis. Really he has been of great help and his deep insights and comments contribute a lot to this thesis.

In addition , I would like to thank all the staff members of the physics department. Indeed they extended a helping hand wherever I asked them to.

Thanks also due to my family for their patience, encouragement and support during this work. In fact, they kept me stable and productive through out the time of this work.

CONTENTS

LIST OF FIGURE CAPTIONS PAGE

CHAPTER ONE

CHAPTER TWO

CHAPTER THREE

CHAPTER FOUR

SUMMARY

For the last two decades, planar optical waveguides have been studied intensively as sensor elements [1-4]. Optical sensors utilize the modification of chemical measurands to optical properties such as intensity, phase, frequency and polarization of an input optical signal. Optical chemical sensors have immunity to electromagnetic interference, have no danger of ignition, field resistant, small size, safe when used in aggressive environments and mechanically stable [5,6]. Moreover, optical sensors based on integrated optics (IO) add some other advantages as a better control of the light path by the use of optical waveguides, a higher mechanical stability and a reduced size [7]. Such kinds of sensor are useful for highly sensitive analysis and monitoring of hazardous environments.

A waveguide sensor is an evanescent field sensor for which the waveguide mode is the sensing feature. The guided electromagnetic field of the waveguide mode extends as an evanescent field into the cladding and substrate media and senses an effective refractive index of the waveguide. The effective refractive index of the propagating mode depends on the structure parameters, e.g., the guiding layer thickness and dielectric permittivity and magnetic permeability of the media constituting the waveguide. As a result, any change in the refractive index of the covering medium results in a change in the effective refractive index of the guiding mode. The basic sensing principle of the planar waveguide sensor is to measure the changes in the effective refractive index due to changes in the refractive index of the covering medium.

The essential part of a waveguide sensor consists of a high refractive index waveguiding film sandwiched between a substrate and the sample

medium to be analyzed, sometimes called the "analyte". In most cases the substrate is a solid material, which has a refractive index lager than that of the analyte. Such a sensor is called normal symmetry sensor. For the sake of power enhancement in the covering medium and hence sensitivity enhancement, sensors of reverse configurations were introduced [8,9] for which the refractive index of the substrate is chosen to be less than that of the analyte. The recent introduction of reverse symmetry waveguides has resulted in high sensitivity sensors.

Optical evanescent wave sensors have been widely used for various purposes such as humidity sensing [10,11], chemical sensing [6,12], biochemical sensing [13,14] and biosensing [15].

O. Parriaux et al. [16-20] presented an extensive theoretical analysis for the design of evanescent linear waveguide sensors and derived the conditions for the maximum achievable sensitivity for both transverse electric (TE) and transverse magnetic (TM) polarizations. R. Horvath et al. [8, 9, 15] demonstrated the design and implementation of a waveguide sensor configuration called reverse-symmetry in which the refractive index of the aqueous cladding is higher than that of the substrate material. The reverse symmetry waveguide has been tested for bacterial and cell detection and it showed a considerable high sensitivity compared with the conventional waveguide sensor. Optical waveguide sensors utilizing surface plasmon resonance (SPR) phenomenon have been studied [21-23]. SPR sensor consists of a four layer structure: a substrate, a guiding layer, a metal layer, and the analyte as a cladding. SPR sensors have been found to have relatively high sensitivity in chemical and biological sensing due to the strong localization of the electromagnetic field. Another type of optical sensors based on an Anti-Resonant Reflecting Optical Waveguide

(ARROW) was presented [24,25]. ARROW sensor generally includes four layers or more. The simplest one comprises a substrate, a film, a first cladding, and a second cladding. In these waveguides the field is confined by two cladding layers on either side of the film form high-reflectivity Fabry-Perot mirrors. M. Shabat et al. [26-28] have investigated the sensitivity of nonlinear waveguide structure where one or more of the layers of the waveguide structure are considered to be nonlinear medium.

The main aim of this thesis is to propose novel planar optical waveguide sensors utilizing a new type of metamaterials called Left-Handed Materials with simultaneously negative electric permittivity and negative magnetic permeability.

This thesis is divided into five chapters starting in chapter one with a basic introduction to electromagnetic theory, concepts of planar waveguides, and fundamental equations required for analyzing slab waveguides.

In chapter two we investigate history, properties, and applications of Left-Handed Materials. We also explore the basic effect of optical waveguide sensor. A three-layer conventional linear sensor is presented.

In chapter three TE polarized waves in a Left-Handed material as a guiding layer surrounded by a nonlinear clad and a linear substrate are presented for sensing application with a focus on the sensitivity of the sensor. The variation of the sensitivity with different parameters of the structure is plotted and explained. The optimum structure that corresponds to the highest sensitivity is also provided.

In chapter four p-polarized waves (TM) are considered to flow in the same waveguide structure presented in chapter three. The sensing sensitivity is derived and plotted with different structure parameters. Power flow through the waveguides layers and its relation with the sensitivity i s presented.

At the end of the thesis, chapter five presents conclusion remarks for the whole work.

CHAPTER ONE
BASIC WAVEGUIDE EQUATIONS

This chapter is intended to establish the fundamental concepts and the basic background of guided waves. It also presents the basic equations needed to analyze optical slab waveguide structure. A brief review of Maxwell's equations, wave equation, total internal reflection, and power considerations is given. The concepts of TE and TM polarizations and waveguide modes are also presented.

1.1 Introduction:

The analysis of dielectric waveguides requires the understanding of electromagnetic field theory in dielectric media. Maxwell developed the electromagnetic theory of light and the kinetic theory of gases. Maxwell's successful interpretation of electromagnetic field resulted in four field equations that bear his name. Maxwell's equations predict the existence of electromagnetic waves that propagate through space at the speed of light c [29,30]. The discovery of electromagnetic waves has led to many practical communication systems, including radio, television, radar, and optoelectronics [31]. On the conceptual level, Maxwell unified the subject of light and electromagnetism by developing the idea that light is a form of electromagnetic radiation.

Electromagnetic waves are transverse waves. They are generated by time-varying currents and charges. Once created, these waves continue to move with a finite velocity independent of the source that produced them.

They carry energy and momentum and hence can exert pressure on a surface.

1.2 Maxwell's Equations:

The governing equations for the electric and magnetic fields are well known over a century ago. Before Maxwell began his work in the field of electromagnetic theory, these equations are written as [29-31]:

$$\oint_l \mathbf{E}' \cdot d\mathbf{l} = emf = -\int_s \frac{\partial \mathbf{B}'}{\partial t} \cdot d\mathbf{s} \quad \text{(Faraday's law)} \tag{1-1}$$

$$\oint_l \mathbf{H}' \cdot d\mathbf{l} = I_{enc} = \int_s \mathbf{J}' \cdot d\mathbf{s} \quad \text{(Ampere's law)} \tag{1-2}$$

$$\oint_s \mathbf{D}' \cdot d\mathbf{s} = Q_{enc} = \int_v \rho_v dv \quad \text{(Gauss's law)} \tag{1-3}$$

$$\oint_s \mathbf{B}' \cdot d\mathbf{s} = 0 \quad \text{(conservation of magnetic flux)} \tag{1-4}$$

where **E'** is the electric field intensity, **H'** the magnetic field intensity, **D'** the electric flux density or electric displacement vector, and **B'** the magnetic flux density. The parameter ρ_v is the volume charge density and **J'** is the electric current density. The notation used above, **E'**, **H'**,… denotes general time varying fields. We will use the notations **E**, **H**, … later for the complex vector fields that are function of space coordinates only. The flux densities **D'** and **B'** and the current density **J'** are related to the fields **E'** and **H'** by the constitutive relations. For linear, isotropic and homogeneous media, the constitutive relations are given by:

$$\mathbf{D}' = \varepsilon \mathbf{E}', \ \mathbf{B}' = \mu \mathbf{H}', \ \mathbf{J}' = \sigma \mathbf{E}', \tag{1-5}$$

where ε, μ and σ is the dielectric permittivity, the magnetic permeability and the conductivity of the medium respectively.

Eq. (1-2) represents Ampere's law for time-invariant currents. To be valid for time-varying currents, we must replace **J'** in it by ($\mathbf{J}' + \partial \mathbf{D}' / \partial t$) [29,30], so that the generalized form of Ampere's law has the form:

$$\oint_l \mathbf{H}'.d\mathbf{l} = \int_s (\mathbf{J}' + \frac{\partial \mathbf{D}'}{\partial t}).d\mathbf{s} \qquad (1\text{-}6)$$

This is the fundamental contribution of Maxwell, which can be interpreted as follows: the displacement current produces a magnetic field according to the same law as normal current.

Eqs. (1-1), (1-3), (1-4), and (1-6) are called Maxwell's equations in integral form. Recalling Stokes's and the divergence theorems: for any vector **A**, we have:

$$\oint_l \mathbf{A} \,.\, d\mathbf{l} = \int_s \nabla \times \mathbf{A} \,.\, d\mathbf{s} \qquad \text{(Stokes's theorem)} \qquad (1\text{-}7)$$

and

$$\oint_s \mathbf{A} \,.\, d\mathbf{s} = \int_v \nabla \,.\, \mathbf{A}\, dv \qquad \text{(divergence theorem)} \qquad (1\text{-}8)$$

Applying Stokes's and the divergence theorems to Maxwell's equations in integral form given by Eqs. (1-1), (1-3), (1-4) and (1-6), we get Maxwell's equations in differential form which can be written as:

$$\nabla \times \mathbf{E}' = -\frac{\partial \mathbf{B}'}{\partial t} \qquad (1\text{-}9)$$

$$\nabla \times \mathbf{H}' = \mathbf{J}' + \frac{\partial \mathbf{D}'}{\partial t} \qquad (1\text{-}10)$$

$$\nabla \,.\, \mathbf{D}' = \rho_v \qquad (1\text{-}11)$$

$$\nabla \,.\, \mathbf{B}' = 0 \qquad (1\text{-}12)$$

We can specialize Maxwell's equations for the type of media we will be faced with when treating dielectric waveguides [31]. For charge free lossless media, where ρ_v and **J'** vanish, Maxwell's equations have the form:

$$\nabla \times \mathbf{E}' = -\frac{\partial \mathbf{B}'}{\partial t} \qquad (1\text{-}13)$$

$$\nabla \times \mathbf{H}' = \frac{\partial \mathbf{D}'}{\partial t} \qquad (1\text{-}14)$$

$$\nabla \,.\, \mathbf{D}' = 0 \qquad (1\text{-}15)$$

$$\nabla \,.\, \mathbf{B}' = 0 \qquad (1\text{-}16)$$

To derive the wave equation of **E'** we take the curl of Eq. (1-13) and make use of the constitutive relation $\mathbf{B}' = \mu\,\mathbf{H}'$, we get:

$$\nabla \times \nabla \times \mathbf{E}' = -\mu\,\frac{\partial \nabla \times \mathbf{H}'}{\partial t} \qquad (1\text{-}17)$$

Using the vector identity

$$\nabla \times \nabla \times \mathbf{A} = \nabla(\nabla \,.\, \mathbf{A}) - \nabla^2 \mathbf{A} \qquad (1\text{-}18)$$

and considering Eqs. (1-14) and (1-15) and the constitutive relation $\mathbf{D}' = \varepsilon\,\mathbf{E}'$, we obtain a plane wave equation in a homogeneous medium as:

$$\nabla^2 \mathbf{E}' - \mu\,\varepsilon\,\frac{\partial^2 \mathbf{E}'}{\partial t^2} = 0 \qquad (1\text{-}19)$$

Taking the curl of Eq. (1-14) and then substituting Eqs. (1-13) and (1-16) leads to the wave equation for H' similar to (1-19) as:

$$\nabla^2 \mathbf{H}' - \mu\,\varepsilon\,\frac{\partial^2 \mathbf{H}'}{\partial t^2} = 0 \qquad (1\text{-}20)$$

1.3 Time Harmonic Fields

Suppose that we have fields that vary sinusoidally in time as [31]:

$$\mathbf{E}'(x,y,z,t) = \mathrm{Re}(\mathbf{E}e^{j\omega t}) \qquad (1\text{-}21)$$

$$\mathbf{H}'(x,y,z,t) = \mathrm{Re}(\mathbf{H}e^{j\omega t}) \qquad (1\text{-}22)$$

$$\mathbf{D}'(x,y,z,t) = \mathrm{Re}(\mathbf{D}e^{j\omega t}) \qquad (1\text{-}23)$$

$$\mathbf{B}'(x,y,z,t) = \mathrm{Re}(\mathbf{B}e^{j\omega t}) \qquad (1\text{-}24)$$

Where ω is the angular frequency.

We are now able to work directly with space coordinate-dependent vectors **E**, **H**, **D**, and **B**.

To write Maxwell's equations for time harmonic fields which called sinusoidal steady state Maxwell's equations, we take the explicit derivative of **B'** and **D'** with respect to time. Eqs. (1-13) – (1-16) can be rewritten as:

$$\nabla \times \mathbf{E} = -j\omega\,\mu\,\mathbf{H} \qquad (1\text{-}25)$$

$$\nabla \times \mathbf{H} = j\omega\,\varepsilon\,\mathbf{E} \qquad (1\text{-}26)$$

$$\nabla \,.\, \mathbf{E} = 0 \qquad (1\text{-}27)$$

$$\nabla \,.\, \mathbf{H} = 0 \qquad (1\text{-}28)$$

Eqs. (1-25) to (1-28) represent Maxwell's equations for time harmonic fields in free charge lossless media.

Taking the curl of Eqs. (1-25) and (1-26), we get Helmholtz equations,

$$\nabla^2\mathbf{E} + \omega^2\mu\,\varepsilon\,\mathbf{E} = 0 \qquad (1\text{-}29)$$

$$\nabla^2\mathbf{H} + \omega^2\mu\,\varepsilon\,\mathbf{H} = 0 \qquad (1\text{-}30)$$

Eqs. (1-29) and (1-30) are called *Helmholtz equations or wave equations* for time harmonic fields.

1.4 Theory of Waveguides:

The simplest optical waveguide structure is the step-index planar slab waveguide. The slab waveguide, shown in Fig. 1-1, consists of a high-refractive index dielectric guiding layer, sometimes called the film, surrounded by two lower-refractive index materials. The slab is infinite in extent in the *yz* plane, but finite in the *x* direction. The refractive index of the film, n_f, must be larger than that of the cover material (cladding), n_c, and the substrate material, n_s, in order for total internal reflection to occur at the interfaces. The refractive index of the cladding is always less than that of the substrate, a case which is called the conventional case. When the cladding and the substrate have the same refractive index, the waveguide is called symmetric; otherwise the waveguide is called asymmetric. The symmetric waveguide is a special case of the asymmetric waveguide. The slab waveguide is clearly an idealization of real waveguides, because real waveguides are not infinite in width [32].

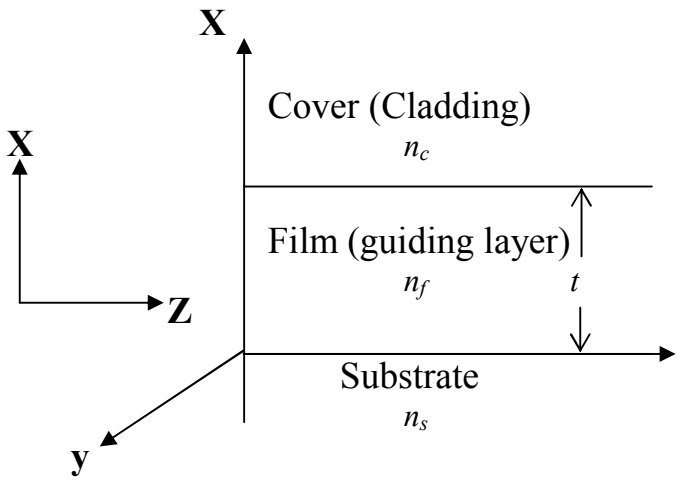

Figure 1.1. Planar slab waveguide consisting of a thin film of thickness t and refractive index n_f, sandwiched between cover and substrate materials with indices n_c and n_s.

1.4.1 Total internal reflection:

An important physical process in guided wave optics is total internal reflection. An understanding of the topic of total internal reflection of an incident wave at a plane dielectric boundary gives one important physical insight into the operation of a dielectric waveguide. The principle of optical confinement into a waveguide is based upon the phenomenon of total internal reflection [33]. To illustrate the concept of total internal reflection we consider an obliquely incident wave upon a boundary going from a denser medium of refractive index n_1 to a less dense medium of refractive index n_2 as shown in Fig. 1.2.

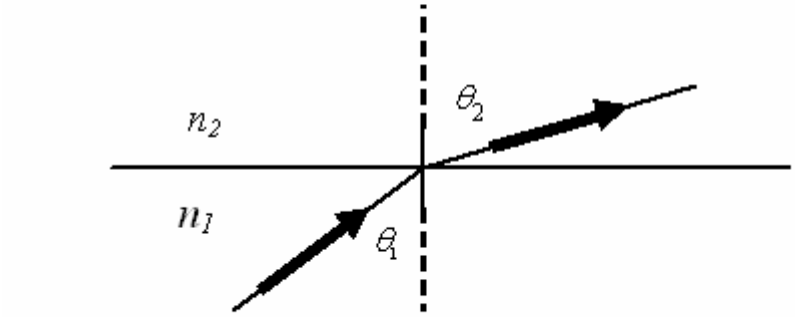

Figure 1.2. Transmission of a light beam going from a denser medium of refractive index n_1 to a rarer medium of index n_2

Total internal reflection will occur at certain angles of incidence greater than an angle known as the critical angle. The angle of transmission θ2 is related to the angle of incidence by Snell's law [33,34]:

$$\frac{\sin(\theta_1)}{\sin(\theta_2)} = \frac{k_2}{k_1} = \frac{\omega\sqrt{\mu_2 \varepsilon_2}}{\omega\sqrt{\mu_1 \varepsilon_1}} = \frac{n_2}{n_1} \qquad (1\text{-}31)$$

Where $k = \frac{2\pi}{\lambda} = \frac{\omega}{c}$ is the propagation constant

We here consider nonmagnetic materials for which $\mu_1 = \mu_2 = \mu_0$. For $n_1 > n_2$ as we increase θ_1 we will reach an angle $\theta_1 = \theta_c$ where $\theta_2 = \pi/2$, that is:

$$\sin(\theta_c) = \frac{n_2}{n_1} \qquad (1\text{-}32)$$

For angles of incidence greater than θ_c, total internal reflection occurs, i.e., no propagating wave in medium 2 and hence the wave will be totally internally reflected in medium 1. The light beam, once it is totally internally reflected, is trapped and confined in the guiding layer. This case corresponds to a guided mode of propagation [35].

1.4.2 Basic equations

Consider the general waveguide structure shown in Fig 1.3. Our purpose in this section is to develop the mathematical model that will enable us to analyze and design a waveguide structure. This general model can be applied to obtain the "modes" in a dielectric slab waveguide and in a round optical fiber. A mode is an allowable field configuration, for a given waveguide geometry, that satisfies Maxwell's equations (or the derived wave equations) and all of the boundary conditions of the fields.

Our wave optics model will yield a complete description of the fields, that is, expressions for the amplitude and components of the propagation vector of the fields associated with a mode.

We will assume that our design objective is to create a dielectric waveguide that propagates energy in a given direction. We define the longitudinal axis of our waveguide as the z axis and design it such that energy is propagating in the guide in the z direction with a longitudinal

propagation constant β (β is the longitudinal component of propagation vector **k**). We will assume that the permittivity $\varepsilon(x, y)$ does not depend on z but can vary with x and y. This special case of an inhomogeneous medium in which ε is independent of one space coordinates is an excellent representation of an optical fiber.

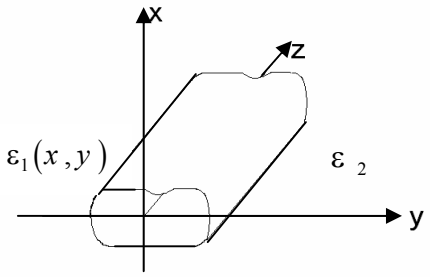

Figure 1.3. An arbitrary-shaped waveguide structure in which the *z*-axis serves as the longitudinal axis.

The expanded form of Eq. (1-25) gives;

$$\left.\begin{aligned} \frac{\partial E_z}{\partial y} - \frac{\partial E_y}{\partial z} &= -j\omega\mu H_x \\ \frac{\partial E_x}{\partial z} - \frac{\partial E_z}{\partial x} &= -j\omega\mu H_y \\ \frac{\partial E_y}{\partial x} - \frac{\partial E_x}{\partial y} &= -j\omega\mu H_z \end{aligned}\right\} \qquad (1\text{-}33)$$

In a similar manner, the expanded form of Eq. (1-26) gives;

$$\left.\begin{aligned} \frac{\partial H_z}{\partial y} - \frac{\partial H_y}{\partial z} &= j\omega\varepsilon E_x \\ \frac{\partial H_x}{\partial z} - \frac{\partial H_z}{\partial x} &= j\omega\varepsilon E_y \\ \frac{\partial H_y}{\partial x} - \frac{\partial H_x}{\partial y} &= j\omega\varepsilon E_z \end{aligned}\right\} \qquad (1\text{-}34)$$

For time harmonic fields, the electric and magnetic fields can be written as:

$$\mathbf{E}(x,y,z,t) = [E_x(x,y)\hat{a}_x + E_y(x,y)\hat{a}_y + E_z(x,y)\hat{a}_z]e^{-j\beta z} \quad (1\text{-}35)$$

$$\mathbf{H}(x,y,z,t) = [H_x(x,y)\hat{a}_x + H_y(x,y)\hat{a}_y + H_z(x,y)\hat{a}_z]e^{-j\beta z} \quad (1\text{-}36)$$

The derivatives with respect to z can be evaluated explicitly. After substituting these derivatives into Eqs. (1-33) and (1-34) and rearranging we can write the transverse components (E_x, E_y, H_x, H_y) in terms of the longitudinal components (E_z, H_z). The result takes the form:

$$E_x = \frac{-j}{\omega^2 \varepsilon \mu - \beta^2}\left(\omega \mu \frac{\partial H_z}{\partial y} + \beta \frac{\partial E_z}{\partial x}\right) \quad (1\text{-}37)$$

$$E_y = \frac{-j}{\omega^2 \varepsilon \mu - \beta^2}\left(\beta \frac{\partial E_z}{\partial y} - \omega \mu \frac{\partial H_z}{\partial x}\right) \quad (1\text{-}38)$$

$$H_x = \frac{-j}{\omega^2 \varepsilon \mu - \beta^2}\left(\beta \frac{\partial H_z}{\partial x} - \omega \varepsilon \frac{\partial E_z}{\partial y}\right) \quad (1\text{-}39)$$

$$H_y = \frac{-j}{\omega^2 \varepsilon \mu - \beta^2}\left(\beta \frac{\partial H_z}{\partial y} + \omega \varepsilon \frac{\partial E_z}{\partial x}\right) \quad (1\text{-}40)$$

The waves in the slab waveguide will be traveling in the *z*- direction. The guide is infinitely extended in the *y* direction. As a result of this infite extension, there is no variation in the field distributions in the *y* direction [31].

Mathematically the limitation imposed by the waveguide symmetry can be expressed as $\frac{\partial}{\partial y} = 0$. Then Eqs. (1-37) to (1-40) can be rewritten as:

$$E_x = \frac{-j\beta}{\omega^2 \varepsilon \mu - \beta^2}\left(\frac{\partial E_z}{\partial x}\right) \quad (1\text{-}41)$$

$$E_y = \frac{j\omega\mu}{\omega^2 \varepsilon\, \mu - \beta^2}\left(\frac{\partial H_z}{\partial x}\right) \tag{1-42}$$

$$E_y = \frac{j\omega\mu}{\omega^2 \varepsilon\, \mu - \beta^2}\left(\frac{\partial H_z}{\partial x}\right) \tag{1-43}$$

$$H_y = \frac{-j\omega\varepsilon}{\omega^2 \varepsilon\, \mu - \beta^2}\left(\frac{\partial E_z}{\partial x}\right) \tag{1-44}$$

1.4.3 Modes of planar slab waveguides:

There are different types of field patterns or configurations inside a waveguide. Each of these distinct field patterns is called a mode. There are two important modes in the analysis of slab waveguides.

1. When $E_z = 0$ and $H_z \neq 0$, this solution corresponds to a transverse electric wave (TE).
2. When $E_z \neq 0$ and $H_z = 0$, this solution corresponds to a transverse magnetic wave (TM).

1.4.3.1 Transverse electric field (TE)

For TE waves, $E_z = 0$ and $H_z \neq 0$. Using Eqs. (1-41) to (1-44) to find the nonzero field component. Only three components exist for TE modes: E_y, H_x, and H_z. The electric and magnetic field can be written as:

$$\mathbf{E}(x,z) = [E_y(x)\hat{a}_y]e^{-j\beta z} \tag{1-45}$$

$$\mathbf{H}(x,z) = [H_x(x)\hat{a}_x + H_z(x)\hat{a}_z]e^{-j\beta z} \tag{1-46}$$

and Helmholtz equation given Eq. (1-29) can be modified to have the form:

$$\frac{\partial^2 E_y}{\partial x^2} + (\omega^2 \mu\, \varepsilon - \beta^2)E_y = 0 \tag{1-47}$$

The nonzero components of the magnetic field as a function of E_y can be written as:

$$H_x = \frac{-\beta}{\omega\ \mu} E_y \tag{1-48}$$

$$H_z = \frac{j}{\omega\ \mu} \frac{\partial E_y}{\partial x} \tag{1-49}$$

1.4.3.2 Transverse magnetic field (TM)

For TM waves, $H_z = 0$ and $E_z \neq 0$. The nonzero field components for this mode are H_y, E_x, and E_z. The electric and magnetic field can be written as:

$$\mathbf{E}(x,z) = [E_x(x)\hat{a}_x + E_z(x)\hat{a}_z]e^{-j\beta z} \tag{1-50}$$

$$\mathbf{H}(x,z) = [H_y(x)\hat{a}_y]e^{-j\beta z} \tag{1-51}$$

In this case, the wave equation (Helmholtz equation) for **H** is similar to Eq. (1-47) with H_y replaces E_y.

E_z and E_x can be written in terms of H_y as:

$$E_x = \frac{\beta}{\omega\ \varepsilon} H_y \tag{1-52}$$

$$E_z = \frac{-j}{\omega\ \varepsilon} \frac{\partial H_y}{\partial x} \tag{1-53}$$

1.4.4 Power Considerations

A useful concept for characterizing electromagnetic waves is the measure of power flowing through a surface. This quantity is called Poynting vector, defined as:

$$\mathbf{S} = \mathbf{E}' \times \mathbf{H}' \qquad (1\text{-}54)$$

It represents the instantaneous intensity (W/m^2) of the wave. The Poynting vector points in the direction of power flow, which is perpendicular to both **E** and **H** fields. The time average intensity for a harmonic field is often given using phasor notation [32]:

$$\langle \mathbf{S} \rangle = \frac{1}{2} \mathrm{Re}[\mathbf{E} \times \mathbf{H}^*], \qquad (1\text{-}55)$$

where Re is the real part and **H*** is the complex conjugate of **H**. The total electromagnetic power moving into a volume is determined by a surface integral of the Poynting vector over the entire area bounding the volume.

Thus, for TE modes we have:

$$\langle \mathbf{S} \rangle = \frac{\beta}{2\,\omega\,\mu} \left| E_y \right|^2 \hat{a}_z \qquad (1\text{-}56)$$

In a similar manner for TM waves

$$\langle \mathbf{S} \rangle = \frac{\beta}{2\,\omega\,\varepsilon} \left| H_y \right|^2 \hat{a}_z \qquad (1\text{-}57)$$

For a multilayer waveguide, the power flowing through the structure can be evaluated using:

$$P_{total} = \frac{\beta}{2\,\omega} \int_{-\infty}^{\infty} \frac{\left|E_y(x)\right|^2}{\mu(x)}\, dx \;\text{; for TE waves} \qquad (1\text{-}58)$$

and

$$P_{total} = \frac{\beta}{2\,\omega} \int_{-\infty}^{\infty} \frac{\left|H_y(x)\right|^2}{\varepsilon(x)}\, dx \;\text{; for TM waves} \qquad (1\text{-}59)$$

CHAPTER TWO
OPTICAL SENSING AND METAMATERIALS

In this chapter we present an overview of materials with negative electric permittivity and negative magnetic permeability. The differences between theses materials and natural materials are discussed. The non-communication application of optical slab waveguides as optical sensors is also presented.

2.1 INTODUCTION

Materials with simultaneously negative permittivity ε and negative permeability μ are called Metamaterials (MTMs). These materials are not naturally occurring materials but were made by composing an array of metallic wire and split ring resonators. A substantial amount of research has been made in different phases for both fundamental electromagnetic and practical applications of these unusual materials in different frequency ranges from radio to optical frequencies. Unusual electromagnetic phenomena of MTMs had been predicted theoretically by Veselago such as reversals of Doppler shift and the Vavilov-Cerenkov effects, reversal of radiation pressure to radiation tension, and negative refraction [36]. All of these phenomena are direct results of the group velocity inversion of electromagnetic waves propagating in such media. For this reason, Veselago named the MTMs as left handed material (LHM).

2.2 OPTICAL SENSING

One of the most important applications of planar waveguides is waveguide sensors. Sensing is performed by the evanescent field in the covering medium [16,23]. The effective refractive index of a waveguide structure depends on film thickness and refractive indices of both film and surroundings. Thus if the chemical or biological changes result in changing the effective refractive index, then the new properties give information about the refractive index of the analyte or the thickness of the adsorbed layer. Sensing process is then the measure of change in effective index due to either changes in cover refractive index or adding an ultra-thin film on surface of the guiding film.

Optical sensor is the noncommunication application field where integrated optic technology is expected to play an increasing role and where it is already successful commercially [17]. The type which is most currently used is the slab structure with a step-index profile. The sensing is performed by the evanescent tail of the modal field in the cover medium. This sensing operation consists of measuring the change of the effective index of a propagating mode when a change of refractive index takes place in the cover. The waveguide characteristic equation or/and a calibration allows the retrieval of the index change from the measured change of the effective index. The sensitivity of the measurement of physical or chemical quantity present in the cover depends on the strength and the distribution of the evanescent field in the cover. The main design task is therefore to find the waveguide structure which maximizes the sensitivity on the quantity to be measured. The analysis differs somewhat if the measurand is homogeneously distributed in the cover (afterwards refered to as homogeneous sensing) or it is an ultra thin film at the waveguide–cover interface (surface sensing). The two cases are illustrated schematically in

Fig.2.1. It is assumed hereafter that the cover medium is a liquid or a gas, which implies that the contact zone between the cover and the waveguide surface is of zero thickness and does not exhibit an air film or bubbles. So far, planar evanescent-guided wave sensors have mostly been used for the detection of ultrathin biological molecular layers immobilized on the surface of a guiding layer (surface sensing). Such a sensing scheme is currently the subject of keen interest in pharmaceutical such as imunoassays. It is also of interest in chemical sensing schemes where the opto-chemical transducing mechanism involves an ultrathin surface layer. The sensitivity in such a configuration, illustrated in Fig.2.1(b), is related to the squared field magnitude at the waveguide-cover interface. Optimizing the sensor sensitivity requires a suitable choice of the waveguide and substrate index n_f and n_s, respectively, as will as the waveguide thickness t relative to the wavelength λ, which maximize the squared modal field at the surface. Evanescent wave sensing of a chemical or physical quantity which is homogeneously distributed in the semi-infinite waveguide cover (homogeneous sensing) refers to a different electromagnetic condition. The sensitivity is now related to the integral of the squared evanescent field in the cover material. This sensing scheme is used in concentration monitoring, for measuring traces of chemicals by means of a thick selective membrane, and, more generally, for measuring all physical/ chemical quantities whose variation corresponds to a change of index.

Optical sensing, in general, is any method by which information that occurs as variations in the intensity, or some other property, of light is translated into an electric signal. This is usually accomplished by the use of various photoelectric devices. In one method, known as optical character recognition, a computer is given the capability of “reading”

printed characters. Reflected or transmitted light from the character strikes an array of photoelectric cells, which effectively dissect it into light and dark areas. By analysis of these areas the computer is able to recognize the character, with some tolerance for less than perfect and uniform printing. Optical sensing is also used in various pattern-recognition systems, e.g., in military reconnaissance and astronomical observation; it is also used in photographic development, to enhance detail and contrast.

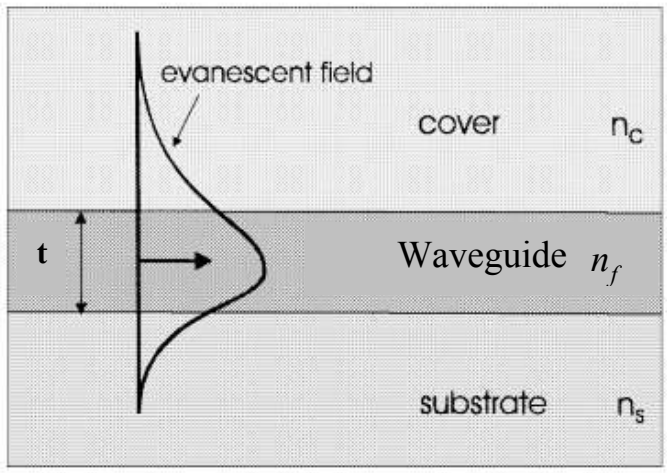

(a)

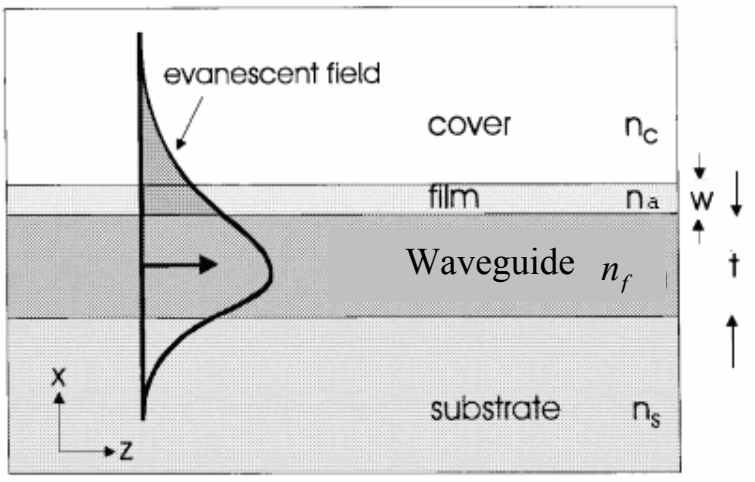

(b)

Fig. 2.1. Schematic representation of (a) slab waveguide homogeneous sensor and (b) surface sensor.

2.2.1 Uses and applications

Planar optical waveguide sensors are used in many aspects: detecting and measuring the thickness of any layers such as metals, metal compounds, organic, bio-organic, enzymes, antibodies and microbes. They are also used in measuring concentrations of liquids and detecting small traces in chemicals.

One of the important uses of such sensors is in radiation dosimeters and protective masks or clothing when they can readily identify and give scanning data about any change in exposure or lack in protection. They are of great benefit in detecting drug vapors. More specifically, planar optical sensors are also used in any chemical, biological or physical processes accompanied with changes in strength and distribution of the evanescent field strength.

2.2.2 Homogeneous sensing

If the properties are homogeneously distributed in the waveguide cover, then the process of detecting changes of these properties is called homogeneous sensing.

Here sensitivity is defined as the change in the effective refractive index through the cover medium, $S = \frac{\partial n_e}{\partial n_c}$ [17].

2.2.3 Surface sensing

If changes of optical properties are due to adsorption of some molecules that construct an ultra-thin film on surface of the guiding thin film, then the process of detecting the adsorbed molecules is said to be surface sensing.

In such configurations, the sensor consists of a guiding film over which sets a sensing layer. Electromagnetic waves propagating along the sensing element are attenuated due to the additional adsorbed film or analyte concentration.

Mathematically, surface sensing is defined as the change of effective refractive index with respect to change in adlayer width, $S = \frac{\partial n_e}{\partial w}$ [17].

2.2.4 Sensor modeling and sensitivity optimization

For commercial sensors to be efficient to practical applications, a sensor must accomplish these properties: small size, low price, optical, mechanical and chemical stability, design flexibility that enables higher complexity on one chart and sensitivity as high as possible. Planar waveguide sensors are the choice.

To maximize sensitivity, appropriate choice of sensor layers and waveguide width must be realized so that changes in the effective refractive index are maximum. The wave guiding film is to some extent arbitrary but its width is of great importance. This means that the main task in designing sensors is to find out the waveguide width that maximizes sensitivity**.**

2.3 Metamaterials

A metamaterial (or meta material) is a material that gains its properties from its structure rather than directly from its composition. The first metamaterials were developed by W.E. Kock in the late 1940's with metal-lens antennas and metallic delay lenses. The metamaterial term is most often used when the material has properties not found in naturally-formed substances. The term was coined by Rodger M. Walser of the University of Texas at Austin in 1999, and he defined the term as follows in 2002: macroscopic composites having a manmade, three-dimensional,

periodic cellular architecture designed to produce an optimized combination, not available in nature, of two or more responses to specific excitation.

Metamaterials are of particular importance in electromagnetism (especially optics and photonics), where they are promising for a variety of optical and microwave applications, such as new types of beam steerers, modulators, band-pass filters, lenses, microwave couplers, and antenna radomes.

In order for its structure to affect electromagnetic waves, a metamaterial must have structural features at least as small as the wavelength of the electromagnetic radiation it interacts with. In order for the metamaterial to behave as a homogeneous material accurately described by an effective refractive index, the feature sizes must be much smaller than the wavelength.

Metamaterials usually consist of periodic structures, and thus have many similarities with photonic crystals and frequency selective surfaces. However, these are usually considered to be distinct from metamaterials, as their features are of similar size to the wavelength at which they function, and thus cannot be approximated as a homogeneous material.

A Russian physicist, V. G. Veselago in 1968, theoretically predicted several extraordinary electromagnetic phenomena of materials with simultaneously negative permittivity and permeability [36], which were a sign change of group velocity, reversals of the Doppler and the Vavilov-Cerenkov effects, negative refraction, and a reversal of radiation pressure to radiation tension. However, his ideas were forgotten until the experimental verification was made by Shelby et al. in 2001 [37] because these exotic materials were thought not to exist in nature at all. This

experimental verification of simultaneously negative permittivity and permeability ignited the present explosive research worldwide in various phases for both fundamental electromagnetic phenomena and practical applications of these unusual materials in various frequency ranges from radio to optical frequencies. Usually, these materials are called metamaterials (MTMs). Although the term MTM has not been strictly defined yet, it is generally admitted to refer to an artificially designed electromagnetic structure with unusual electromagnetic properties that are rarely found in nature. “Meta ” is a Greek prefix meaning “beyond, ” so MTMs can be understood as materials that exhibit an extraordinary electromagnetic response . In the MTMs , the directions of the electric field (**E**), the magnetic field (**H**), and the wave propagation vector (**k**) obey the left-hand rule instead of the right-hand rule in ordinary dielectric materials, so MTMs are also commonly refered to as left-handed materials (LHMs) .The reversals of the phase and the energy propagations in MTMs due to the left- handedness lead to backward wave propagations with opposite directions of the phase and the group velocities , i.e., negative phase velocity or negative group velocity. Since refraction is reversed when electromagnetic waves are incident on LHM, they are also called materials with negative refractive index or negative index media. As explained above, LHMs are media with simultaneous negative permittivity and permeability at a given frequency, so they are also called double-negative media. Due to the double negative property, the electromagnetic wave propagations along these exotic media are quite extraordinary.

2.3.1 Negative refractive index

The main reason for investigating metamaterials is the possibility of creating a structure with a negative refractive index because this feature is not a available in natural materials. Almost all materials encountered in

optics, such as glass or water, have positive values for both permittivity ε and permeability μ. However, many metals (such as silver and gold) have negative ε at visible wavelengths. A material having either (but not both) ε or μ negative is opaque to electromagnetic radiation.

Although the optical properties of a transparent material are fully specified by the parameters ε and μ, in practice the refractive index *n* is often used. *n* may be determined from the relation $n = \sqrt{\varepsilon\mu}$. All known transparent materials possess positive values for ε and μ. By convention the positive square root is used for *n*.

However, LHMs have $\varepsilon < 0$ and $\mu < 0$; because the product εμ is positive, *n* is real. Under such circumstances, it is necessary to take the negative square root for *n*. Physicist Victor Veselago proved that such substances can transmit light [36].

Metamaterials with negative *n* have numerous startling properties:

- Snell's law ($n_1 \sin\theta_1 = n_2 \sin\theta_2$) still applies, but as n_2 is negative, the rays will be refracted on the same side of the normal on entering the material.
- The Doppler shift is reversed: that is, a light source moving toward an observer appears to reduce its frequency.
- Cherenkov radiation points the other way.
- The time-averaged Poynting vector is antiparallel to phase velocity. This means that unlike a normal right-handed material, the wave fronts are moving in the opposite direction to the flow of energy.

For plane waves propagating in such metamaterials, the electric field, magnetic field and Poynting vector (or group velocity) follow a left-hand rule.

2.3.2 Theoretical models

Left-handed materials (LHMs) were first introduced theoretically by Victor Veselago in 1968 [36]. J. B. Pendry [37] was the first to theorize a practical way to make a left-handed metamaterial (LHM). Pendry's initial idea was that metallic wires aligned along propagation direction could provide a metamaterial with negative permittivity ($\varepsilon<0$). Note however that natural materials (such as ferroelectrics) were already known to exist with negative permittivity. The challenge was to construct a material that also showed negative permeability ($\mu<0$). In 1999, Pendry demonstrated that an open ring (C-shape) with axis along the propagation direction could provide a negative permeability. In the same paper, he showed that a periodic array of wires and rings could give rise to a negative refractive index.

The analogy is as follows: Natural materials are made of atoms, which are dipoles. These dipoles modify the light velocity by a factor n (the refractive index). The ring and wire units play the role of atomic dipoles: the wire acts as a ferroelectric atom, while the ring acts as an inductor L and the open section as a capacitor C. The ring as a whole therefore acts as a LC circuit. When the electromagnetic field passes through the ring, an induced current is created and the generated field is perpendicular to the magnetic field of the light. The magnetic resonance results in a negative permeability; the index is negative as well.

CHAPTER THREE
CHARACTERISTICS OF TE OPTICAL WAVEGUIDE SENSORS USING LEFT-HANDED MATERIALS

In this chapter, an extensive theoretical analysis of a novel waveguide structure as an optical sensor is carried out. The waveguide sensor structure considered here consists of a Left-Handed material (LHM) as a guiding layer sandwiched between a linear substrate and a nonlinear cladding with an intensity dependent refractive index. The sensitivity of the proposed optical waveguide sensor is derived. The variation of the sensitivity with different parameters of the waveguide structure is studied. The condition needed for the sensor to exhibit the maximum sensitivity is also discussed. This condition allows the designer to find the right dimensions of the proposed structure. Experiments with the above concepts could be demonstrated and carried out for future versatile sensors.

3.1 Introduction:

Optical waveguide sensors are considered as a rapidly growing field of research. Integrated optical waveguides are widely used for designing optical sensors which are very important mainly because of their miniature, high sensitivity, small size, immunity to electromagnetic interference and low price [5,6]. Homogeneous sensing is mainly used in concentration monitoring, measuring traces of chemicals and studying all physical and chemical properties that change in accordance with changes in refractive indices [17]. The type of waveguides currently used in biochemical and medical sensing is the planar optical waveguide structure.

One of the first applications of the Left-Handed materials (LHMs) was reported by Pendry [38], who demonstrated that a slab of a Left-

Handed material (LHM) can provide a perfect image of a point source. A. Grbic et al [39] verified by a simulation the enhancement of evanescent waves in a transmission-line network by using a Left-Handed material (LHM).

3.2 Mathematical Evaluations

3.2.1 Characteristic Equation

The structure of our waveguide sensor is presented in Fig. 3.1 where the waveguide film is embedded into a linear substrate and a nonlinear cover with an intensity dependent refractive index whose dielectric function [40-43] of the electric field is expressed as:

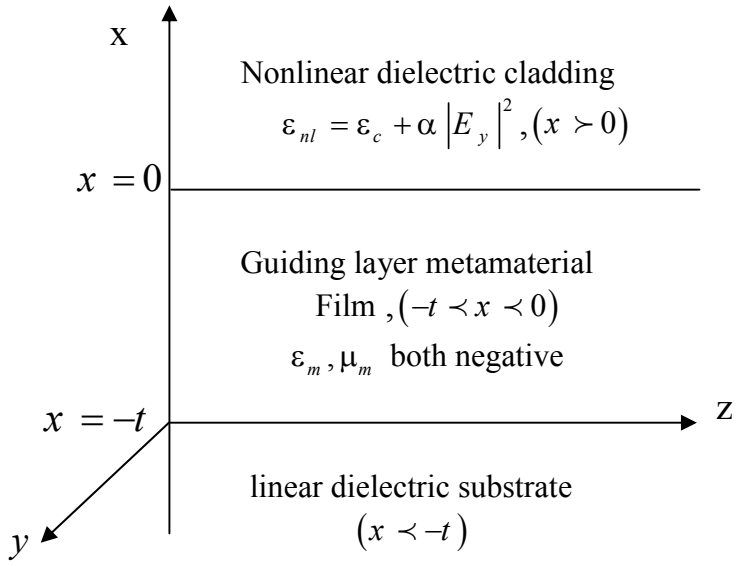

Fig.3.1 :The waveguide structure under consideration

$$\varepsilon_{nl} = \varepsilon_c + \alpha \left|E_y\right|^2 \qquad (3\text{-}1)$$

where $\alpha = \varepsilon_0 \varepsilon_c c n_{2c}$ is the nonlinearity constant, c the speed of light and n_{2c} is the nonlinearity coefficient [41].

The guiding film (*f*) of thickness (*t*) fills the region $-t \le x \le 0$ and the two dielectrics substrate and cladding fill the regions $x < -t$ and $x > 0$, respectively. The waves are assumed to propagate along the *z* axis and guiding surfaces are parallel to the *yz* plane.

The electric field for TE waves propagating in the *z*-direction is expressed as:

$$E = \left(0, E_y, 0\right) e^{j(\omega t - \beta z)} \tag{3-2}$$

where $\beta = k_0 n_e$

Helmholtz equation takes the form:

$$\frac{\partial^2 E_y}{\partial x^2} + (\mu\varepsilon\omega^2 - \beta^2) E_y = 0 \tag{3-3}$$

We assume the cladding and substrate to be non magnetic materials $\mu_c = \mu_s = \mu_0$ where $\mu_r = 1$ is the relative permeability .

Equation (3-3) in the three layers can be written as:

$$\frac{\partial^2 E_{y_1}}{\partial x^2} - k_0^2 (n_e^2 - n_c^2) E_{y_1} + \alpha k_0^2 E_{y_1}^3 = 0, \left(x \succ 0\right); \text{ cladding} \tag{3-4}$$

$$\frac{\partial^2 E_{y_2}}{\partial x^2} + k_0^2 (m n_f^2 - n_e^2) E_{y_2} = 0, \left(-t \prec x \prec 0\right); \text{ film} \tag{3-5}$$

Where $m = \frac{\mu_m}{\mu_0}$ with μ_m and μ_0 are the guiding layer and free space permeabilities respectively.

$$\frac{\partial^2 E_{y_3}}{\partial x^2} - k_0^2 (n_e^2 - n_s^2) E_{y_3} = 0, \left(x \prec -t\right); \text{ substrate} \tag{3-6}$$

For the sake of simplicity we consider:

$$q_c = \sqrt{n_e^2 - n_c^2}, q_s = \sqrt{n_e^2 - n_s^2}, p = \sqrt{m n_f^2 - n_e^2}$$

We solve Helmholtz equations in the three layers to get "E_y" in each layer [41].

$$E_{y_1} = \sqrt{\frac{2}{\alpha}} \frac{q_c}{\cosh[k_0 q_c (x + x_0)]}, \ (x \succ 0) \tag{3-7}$$

where x_0 is a constant related to the power propagating in the waveguide. More specifically, the field peaks at $x = x_o$ [41].

$$E_{y_2} = B_e \cos(k_o p x) + C_e \sin(k_o p x), \ (-t \prec x \prec 0) \tag{3-8}$$

$$E_{y_3} = D_e \exp[k_o q_s (x + t)], \ (x \prec -t) \tag{3-9}$$

The electric field at the clad-film interface is obtained by substituting $x = 0$ in Eq. (3-7), we get $E_o = E_{y_1}(x = 0) = \sqrt{\frac{2}{\alpha}} \frac{q_c}{\cosh(k_o q_c x_o)}$ which can be written as: $\frac{\alpha E_0^2}{2} = q_c^2 (1 - \tanh^2(k_o q_c x_o))$, where $\frac{\alpha E_0^2}{2}$ is called clad-film interface nonlinearity or optical power density at the interface.

Making use of Eqs.(1-48) and (1-49), we can calculate the nonzero components of the magnetic fields.

$$H_{x_1} = \frac{k_0 n_e}{\mu\omega} E_{y_1} = \frac{k_0 n_e}{\mu\omega} \left[\sqrt{\frac{2}{\alpha}} \frac{q_c}{\cosh\left[k_0 q_c (x + x_0)\right]} \right] \tag{3-10}$$

$$H_{x_2} = \frac{k_0 n_e}{\mu\omega} E_{y_2} = \frac{k_0 n_e}{\mu\omega} [B_e \cos(k_0 p x) + C_e \sin(k_0 p x)] \tag{3-11}$$

$$H_{x_3} = \frac{k_0 n_e}{\mu\omega} E_{y_3} = \frac{k_0 n_e D_e}{\mu\omega} \exp\left[k_0 q_s (x + t)\right] \tag{3-12}$$

$$H_{z_1} = \frac{j}{\mu\omega} \frac{\partial E_{y_1}}{\partial x} = \frac{-jk_0}{\mu_0\omega} \sqrt{\frac{2}{\alpha}} q_c^2 \sec h\left[k_0 q_c (x + x_0)\right] \tanh\left[k_0 q_c (x + x_0)\right] \tag{3-13}$$

$$H_{z_2} = \frac{j}{m\mu_0\omega} \frac{\partial E_{y_2}}{\partial x} = \frac{jk_0 p}{m\mu_0\omega} [-B_e \sin(k_0 p x) + C_e \cos(k_0 p x)] \tag{3-14}$$

$$H_{z_3} = \frac{j}{\mu_0\omega} \frac{\partial E_{y_3}}{\partial x} = \frac{jk_0 q_s D_e}{\mu_0\omega} \exp[k_0 q_s (x + t)] \tag{3-15}$$

Applying the Boundary conditions at $x=0$ and $x=-t$. The tangential components E_y and H_z are continuous. The continuity of E_y gives:

$$\sqrt{\frac{2}{\alpha}}\frac{q_c}{\cosh\left[k_0 q_c x_0\right]}=B_e \tag{3-16}$$

$$B_e\cos(k_0 pt)-C_e\sin(k_0 pt)=D_e \tag{3-17}$$

The continuity of H_z gives:

$$-\sqrt{\frac{2}{\alpha}}q_c^2\sec h\left(C\right)\tanh\left(C\right)=\frac{p}{m}C_e \tag{3-18}$$

$$\frac{p}{m}\left[B_e\sin\left(k_0 pt\right)+C_e\cos\left(k_0 pt\right)\right]=q_s D_e \tag{3-19}$$

where $C=k_o q_c x_o$

With some mathematical treatment and rearrangement of Eqs. (3-16) to (3-19) we obtain the characteristic equation;

$$k_0 pt=\tan^{-1}(mx_s)+\tan^{-1}(mx_c\tanh C)+N\pi \tag{3-20}$$

where $x_s=\frac{q_s}{p}$, $x_c=\frac{q_c}{p}$, and $N=0,1,2,\ldots$ is the mode order

It's straight forward to show that x_c and n_e can be written in terms of x_s as:

$$x_c^2=x_s^2\frac{(a_c-m)+(a_c-a_s)}{(a_s-m)},\qquad n_e=\sqrt{\varepsilon_f}\sqrt{\frac{a_s+mx_s^2}{1+x_s^2}} \tag{3-21}$$

where $a_c=\frac{n_c^2}{n_f^2}$ and $a_s=\frac{n_s^2}{n_f^2}$.

3.2.2 Evaluation of the Sensitivity

In homogeneous sensing, sensitivity (S) is defined as the rate of change of the modal effective index $\left(n_e\right)$ with respect to the change of the cover index [27,28], i.e. $S=\frac{\partial n_e}{\partial n_c}$.

Applying this to the characteristic equation given by Eq. (3-20) and after some arrangements, the sensitivity can be expressed as:

$$S = \frac{\sqrt{a_c}\sqrt{1+x_c^2}\left(H_m + \tanh(C)\right)}{x_c\sqrt{a_c + mx_c^2}\left(1+m^2x_c^2\tanh^2(C)\right)\left[\frac{T_e}{m} + \frac{\left(1+x_s^2\right)}{x_s\left(1+m^2x_s^2\right)} + G_e\right]} \qquad (3\text{-}22)$$

Where;

$$H_m = k_0 x_0 x_c \sqrt{\varepsilon_f}\sqrt{\frac{m-a_s}{1+x_s^2}}\left(1-\tanh^2 C\right) \qquad (3\text{-}23)$$

$$T_e = k_0 pt = \tan^{-1}\left(mx_s\right) + \tan^{-1}\left(mx_c\tanh C\right) + N\pi \qquad (3\text{-}24)$$

$$G_e = \frac{H_m + \tanh C\left(1+x_c^2\right)}{x_c\left(1+m^2x_c^2\tanh^2 C\right)} \qquad (3\text{-}25)$$

If the covering medium is linear, then $tamh(C)$ equals 1 and equation (3-22) will coincide with the published results given in literature [17].

3.2.3 The condition of maximum sensitivity

In designing sensors, we seek to bring the sensor to its maximum sensitivity provided a certain configuration. That is at a given configuration of constant $\varepsilon_c, \varepsilon_f$ and ε_s, the condition for maximum sensitivity is achieved when the derivative of S with respect to the guiding layer thickness t vanishes [17,27]. Differentiating Eq. (3-22) with respect to x_s and using the identity $\frac{\partial S}{\partial t} = \frac{\partial S}{\partial x_s}\frac{\partial x_s}{\partial t} = 0$ to obtain the condition of maximum sensing sensitivity. For the sake of simplicity we define :

$$\beta = k_0 x_0 p\left[\omega\frac{x_s}{x_c} - \frac{x_s x_c}{1+x_s^2}\right] \qquad (3\text{-}26)$$

$$\sigma = 1-\tanh^2 C \qquad (3\text{-}27)$$

$$\sigma_1 = \sigma\beta\left[1-2C\tanh C\right] \qquad (3\text{-}28)$$

$$\beta_1 = \frac{m}{1+m^2 x_s^2} + \frac{m x_c \sigma\beta + m \tanh C\left(\omega x_s / x_c\right)}{1+m^2 x_c^2 \tanh^2 C} \tag{3-29}$$

$$G_e = \frac{H_m + \tanh C\left(1+x_c^2\right)}{\left(x_c + m^2 x_c^3 \tanh^2 C\right)} = \frac{H_m + \tanh C\left(1+x_c^2\right)}{x_c \phi} \tag{3-30}$$

$$\gamma = \frac{x_c \phi r_1 - r_2 r_3}{x_c^2 \phi^2} \tag{3-31}$$

$$\phi = 1 + m^2 x_c^2 \tanh^2 C \tag{3-32}$$

$$\omega = \frac{m - a_c}{m - a_s} \tag{3-33}$$

$$r_2 = H_m + \tanh C\left(1+x_c^2\right) \tag{3-34}$$

$$r_1 = \sigma_1 + \tanh C\left(2 x_s \omega\right) + \left(1+x_c^2\right)\sigma\beta \tag{3-35}$$

$$r_3 = \omega \frac{x_s}{x_c} + 2m^2 x_c^3 \tanh C \sigma\beta + 3m^2 \tanh^2 C \omega x_s x_c \tag{3-36}$$

$$\sigma_2 = \frac{2x_s^2\left(1+m^2 x_s^2\right) - \left(1+x_s^2\right)\left(1+3m^2 x_s^2\right)}{x_s^2\left(1+m^2 x_s^2\right)^2} \tag{3-37}$$

The condition now can be written as:

$$\sqrt{a_c}\sqrt{a_c + m x_c^2}\, x_c \phi \sigma_3 \left[\sqrt{1+x_c^2}\left(\sigma_1 + \sigma\beta\right) + \frac{\left(H_m + \tanh C\right)\omega x_s}{\sqrt{1+x_c^2}}\right] \cdot$$
$$\sqrt{a_c}\sqrt{1+x_c^2}\left(H_m + \tanh C\right)\left[\sqrt{a_c + m x_c^2}\, x_c \phi \beta_2 + \sigma_3 \beta_3\right] = 0 \tag{3-38}$$

Where ;

$$\sigma_3 = \frac{T_e}{m} + \frac{1+x_s^2}{x_s\left(1+m^2 x_s^2\right)} + G_e \tag{3-39}$$

$$\beta_2 = \frac{\beta_1}{m} + \sigma_2 + \gamma \tag{3-40}$$

$$\beta_3 = \sqrt{a_c + m x_c^2}\, r_3 + \frac{x_c \phi m \omega x_s}{\sqrt{a_c + m x_c^2}} \tag{3-41}$$

3.2.4 Power flow within the three layers

The energy flux of the guided-wave modes per unit length is given by Eq. (1-58). Applying the power expression given by Eq. (1-58) to the solutions of Helmholtz equation in the three layers given by Eqs. (3-7) to (3-9) .

Carrying out this integration, one can finally have:

$$p_c = \frac{n_e x_c p}{\omega \mu_0 \alpha}\left[1 - \tanh C\right] \tag{3-42}$$

$$p_f = \frac{n_e k_0}{2\omega m \mu_0}\left\{\frac{B_e^2}{2}\left[t - \frac{\sin\left(2k_0 pt\right)}{2k_0 p}\right] + \frac{C_e^2}{2}\left[t + \frac{\sin\left(2k_0 pt\right)}{2k_0 p}\right] + \left[\frac{B_e C_e}{k_0 p}\sin^2\left(k_0 pt\right)\right]\right\} \tag{3-43}$$

$$p_s = \frac{n_e D_e^2}{4\omega \mu_0 x_s p} \tag{3-44}$$

Where ;

$$B_e = \sqrt{\frac{2}{\alpha}}\frac{q_c}{\cosh C} \tag{3-45}$$

$$C_e = -\frac{m}{p}\sqrt{\frac{2}{\alpha}} q_c^2 \sec hC \tanh C \tag{3-46}$$

$$D_e = B_e \cos\left(k_0 pt\right) - C_e \sin\left(k_0 pt\right) \tag{3-47}$$

The total power through the three-layer structure is given by:

$$p_{total} = \frac{n_e}{\omega \mu_0}\left[\frac{x_c p}{\alpha} y_1 + \frac{k_0}{2m}\left\{\frac{B_e^2}{2} x_- + \frac{C_e^2}{2} x_+ + \frac{B_e C_e}{k_0 p}\sin^2(k_0 pt)\right\} + \frac{D_e^2}{4x_s p}\right] \tag{3-48}$$

where ;

$$y_1 = 1 - \tanh C \tag{3-49}$$

$$x_{-} = t - \frac{\sin\left(2k_0 pt\right)}{2k_0 p} \tag{3-50}$$

$$x_{+} = t + \frac{\sin\left(2k_0 pt\right)}{2k_0 p} \tag{3-51}$$

For sensing applications, the most important parameter is the fraction of total power flowing in the cladding which is given by :

$$\frac{P_c}{P_{total}} = \frac{\frac{x_c p}{\alpha} y_1}{\left[\frac{x_c p}{\alpha} y_1 + \frac{k_0}{2m}\left\{\frac{B_e^2}{2} x_{-} + \frac{C_e^2}{2} x_{+} + \frac{B_e C_e}{k_0 p}\sin^2\left(k_0 pt\right)\right\} + \frac{D_e^2}{4x_s p}\right]} \tag{3-52}$$

3.3 Results and Discussion

The mathematical argument above constructs a complete set of equations capable of determining all of the parameters needed for the sensor to exhibit its maximum sensing sensitivity. Given the asymmetry parameters a_c and a_s and substituting for x_s from Eq. (3.21), then Eq. (3-38) turns to be a function of x_c only and is easily solved. Substituting these values in the characteristic equation Eq. (3-20), we can compute the waveguide widths ensuring maximum sensitivity. The values of these maxima are calculated through substituting the last values in the expression of the above sensitivity Eq. (3-22). Plotting these results against a_c and $a_{s,}$ a designer ends with a 3D chart from which all parameters required for maximization of such sensors may be derived [17,27,28].

Although expressions above are valid for any order of TE modes, the discussion to follow is restricted only to the fundamental mode (N =0) which has the highest sensitivity[10].

A typical way to proceed is as follows:

The cover material is chosen according to the proposed usage of the sensor thus giving the refractive index n_c. The choice of substrate

(consequently n_s) is controlled by cost requirements, mechanical stability and temperature. As for the guiding material, chemical and optical stabilities are considered. Thus the optogeometrical parameters a_s and a_c are determined. The designer will look at the chart representing x_s as a function of a_s and a_c to find the value of x_s which provides the highest sensitivity. Introducing the solution found for x_s into Eqs. (3-21) to find the optimum normalized parameter x_c and effective index (n_e).The optimum guiding layer thickness is obtained by substituting these values into the dispersion relation given by Eq. (3-20). Substituting these values into Eq. (3- 22), the maximum sensitivity achievable is calculated.

A computer program was generated using maple 9 to solve the characteristic equation for the effective refractive index and to calculate the sensitivity. This enables us to plot the results and to study the variation of the sensitivity with the different parameters of the structure.

In Figs. 3.2 and 3.3 the sensitivity of the proposed sensor was plotted versus the asymmetry parameter a_c. It is clear that the sensitivity increases with increasing a_c. This is a normal behavior since the sensing operation is performed by the evanescent optical field extending from the thin guiding film into the nonlinear covering medium. To obtain high sensitivity, it is essential to get as much of the optical power as possible to propagate in the nonlinear cladding medium. In this sense, increasing a_c will enhance the power fraction flowing in the cladding. The optimum geometry is expected to be obtained by the so called reverse symmetry waveguides [9,15]. In principle, this configuration allows most of the optical power to present in the covering medium which is contrary to the conventional waveguide geometry, where typically less than 10% of the total power is present in the cladding medium [44]. Despite this fact, we will keep assuming that our system has the normal symmetry because it is the case of most practical

cases and our interest here is dedicated to the effect of nonlinearity on the sensitivity. A comparison between the proposed sensor and the thr ee-layer

linear sensors is shown in Fig. 3.3. As can be seen the proposed sensor is recommended for large values of a_c.

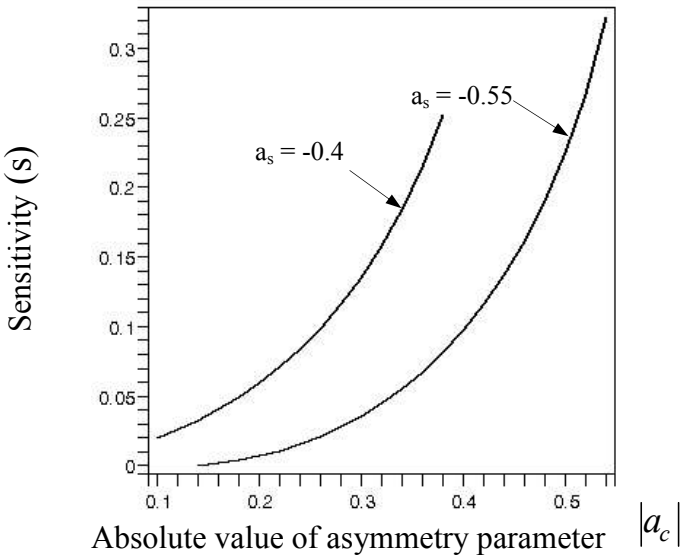

Figure 3.2. Sensitivity versus the absolute value of the asymmetry parameter a_c for the proposed optical waveguide sensor.

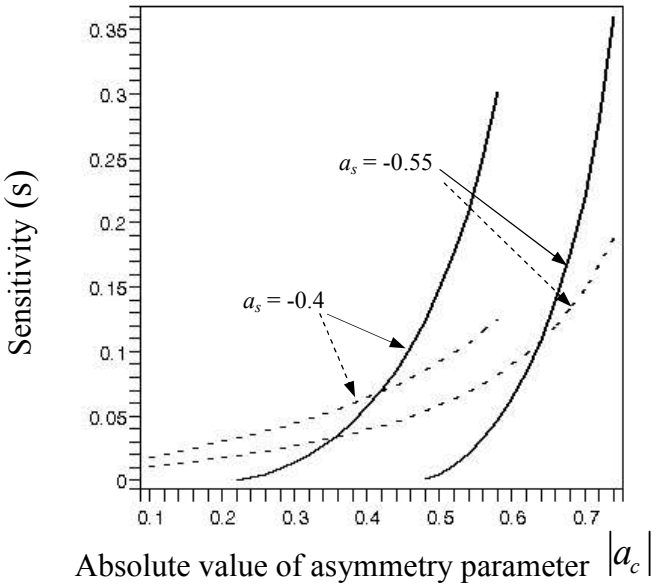

Figure 3.3. Sensitivity with the absolute value of the asymmetry parameter a_c for the proposed sensor (solid line) and for the conventional three-layer sensor (dashed line).

The behavior of the sensitivity with the absolute value of the asymmetry parameter a_s is opposed to that with a_c. Fig. 3.4 shows that the sensitivity of the proposed waveguide configuration decreases with increasing a_s. As a_s increases the evanescent field in the substrate is enhanced thus the part of field in the cladding is reduced. As a result, the sensitivity of the optical sensor decreases.

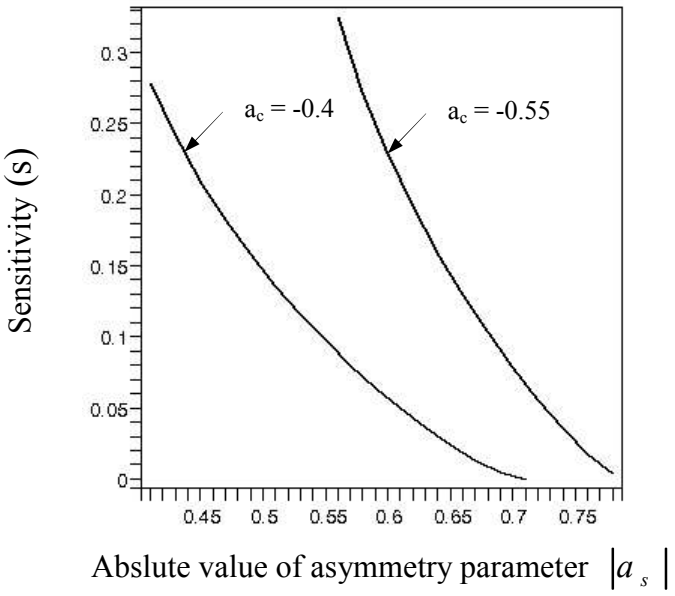

Figure 3.4. Sensitivity versus the absolute value of the asymmetry parameter a_s for the proposed optical waveguide sensor.

Figure 3.5 shows the 3D representation of the condition of maximum sensitivity given by Eq. (3-38) from which the designer can extract the information required to build the optimum structure of the proposed waveguide structure as illustrated at the beginning of this section.

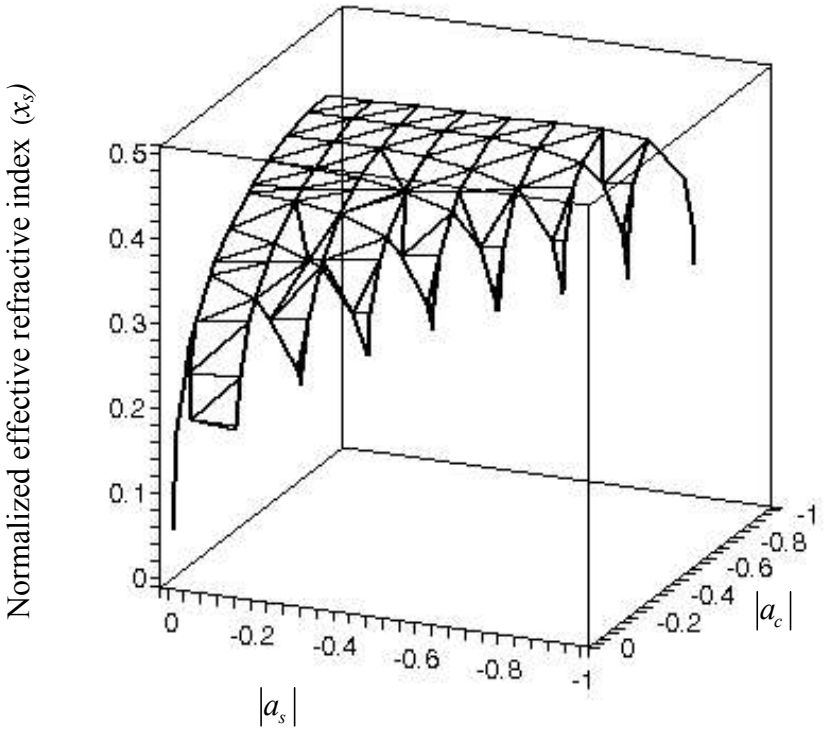

Figure 3.5. Normalized effective refractive index x_s versus a_s and a_c ensuring maximum sensitivity for homogeneous sensing.

In Fig. 3.6 the sensitivity of the proposed sensor is shown as a function of the absolute value of m where $\mu_m = m\mu_o$. As can be seen, for small values of $|m|$ the sensitivity approaches zero due to the high confinement of the guided mode in the guiding layer. In the other limit, all the power of the mode propagates in the substrate. Consequently, the sensor probes the substrate side only and the sensitivity of the effective refractive index to variations in the index tends to zero. Between these two limits, there is a maximum in the sensitivity curves representing an optimum where a relatively large part of the total mode power propagates in the cladding.

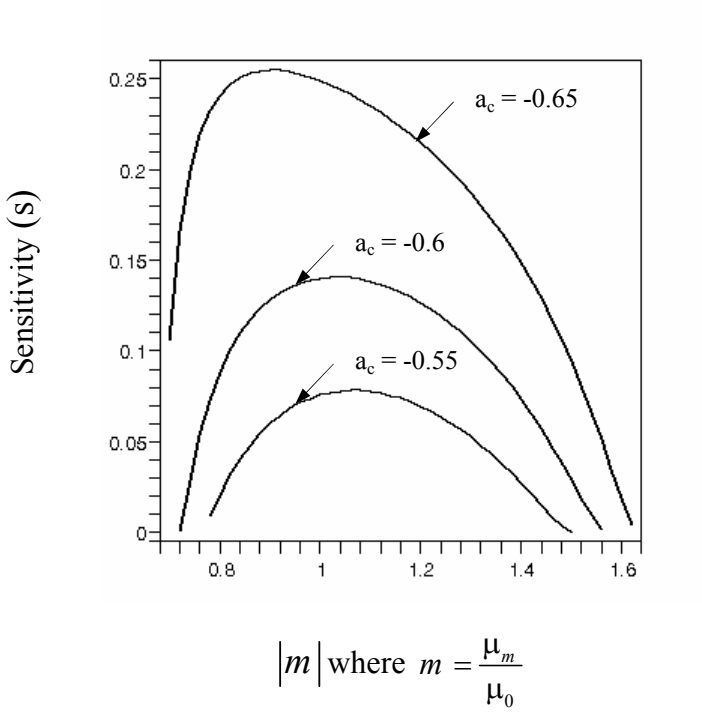

Figure 3.6. Sensitivity of the proposed sensor versus the absolute value of m where $\mu_m = m\mu_o$ for different values of a_c and a_s = -0.67.

The variation of the sensitivity with the term $\tanh C$ which arises from the nonlinearity of the cladding is plotted in Fig. 3.7. As the term $\tanh C$ goes to unity in Eq. (3-20), we obtain the well known characteristic equations for linear waveguides [16]. Fig. 3.7 shows the sensitivity to have its minimum value as $\tanh C$ goes to one, the linear cladding. Thus we conclude an optical sensor with nonlinear cladding can enhance the sensitivity of conventional linear sensors.

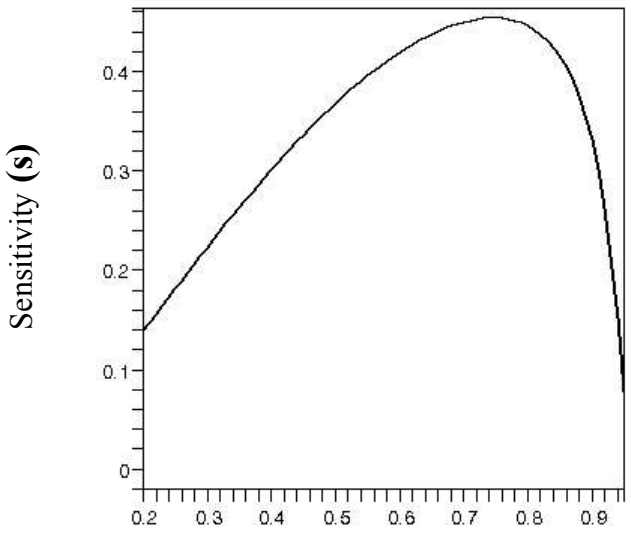

Figure 3.7. Sensitivity of the proposed optical waveguide sensor versus tanhC.

Fig. 3.8 verifies the close connection between the fraction of total power propagating in the cover medium (P_c/P_{total}) and the sensitivity of the sensor. In most cases, they may be regarded as nearly identical to the theoretical consideration thus the enhancement of the fraction of power flowing in the clad is essential for sensing applications.

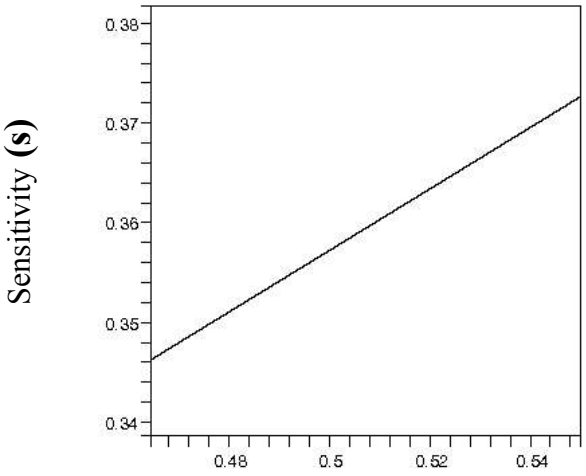

Figure 3.8. Sensitivity of the proposed optical waveguide sensor versus the fraction of total power flowing in the cladding.

Fig. 3.9 shows the sensitivity of the proposed sensor as a function of clad-film interface nonlinearity for a_c = -0.65,a_s = -0.75.. The sensitivity increases with increasing the clad-film interface nonlinearity. This behavior is attributed to the following considerations: as the nonlinear coefficient α increases for self-focused nonlinearity case the permittivity of the cladding increases hence the fraction of total power flowing in the cladding is enhanced. Moreover as the squared field magnitude at the clad-film interface (it represents the intensity at the clad-film interface) increases the evanescent tail in the cladding increases and the sensitivity of the sensor also increases.

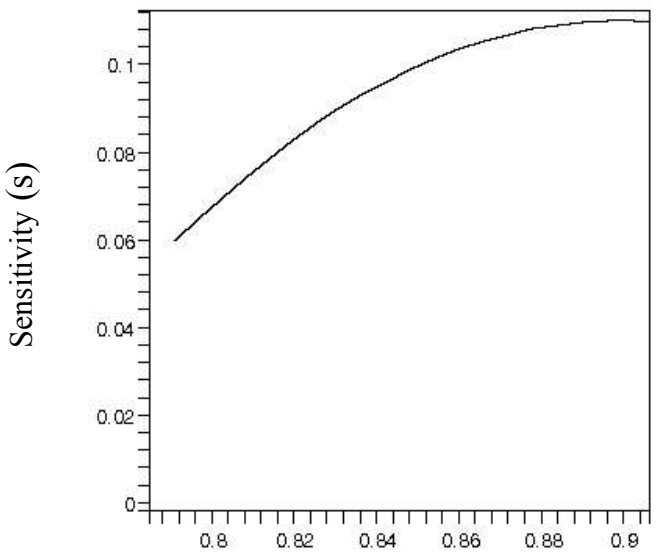

Figure 3.9 Sensitivity versus the clad-film interface nonlinearity for a_c = -0.65, a_s = -0.75.

Finally the resulting sensitivity curve as a function of the permittivity of the LHM as a guiding layer is shown in Fig. 3.10. There is an optimum value of ε_f at which the fraction of total power flowing in the nonlinear cladding is maximum and the sensitivity of the optical waveguide sensor is also maximum.

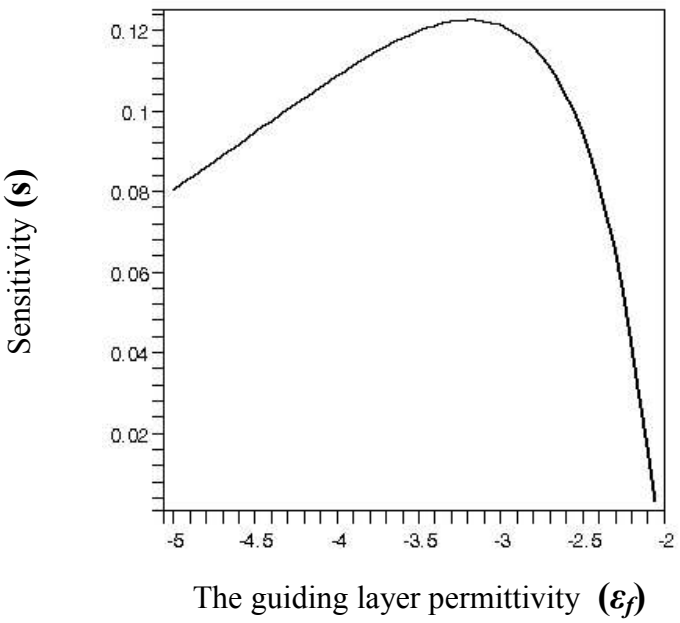

Figure 3.10. Sensitivity of the proposed sensor versus the guiding layer permittivity for t = 100nm, λ = 1550nm, and $\mu_m = -\mu_o$ (m = -1).

CHAPTER FOUR

HOMOGENEOUS TM NONLINEAR WAVEGUIDE SENSORS USING LEFT - HANDED MATERIALS

This chapter is devoted to nonlinear p-polarized waves propagating in a waveguide structure as an optical sensor. Here we consider the structure discussed in chapter three with a different light polarization. Sensitivity of this configuration is discussed and the condition required to maximize the sensing sensitivity is determined. The fraction of total power flowing in the covering medium is shown to be related to sensitivity.

4.1 Dispersion equations

To deduce the dispersion equation, we must first solve Helmholtz equation and determine the form of the fields in each layer of the proposed sensor. The sensor under consideration is a thin metamaterial film sandwiched between a linear substrate and a nonlinear cover with an intensity dependent refractive index. The guiding film fills the region $-t \le x \le 0$ and the two dielectrics substrate and cladding fill the regions x<-t and x>0 respectively. Waves propagate along the z-axis and the guiding surfaces are fabricated parallel to the *yz*-plane. A schematic diagram of this sensor is shown in figure 4.1.

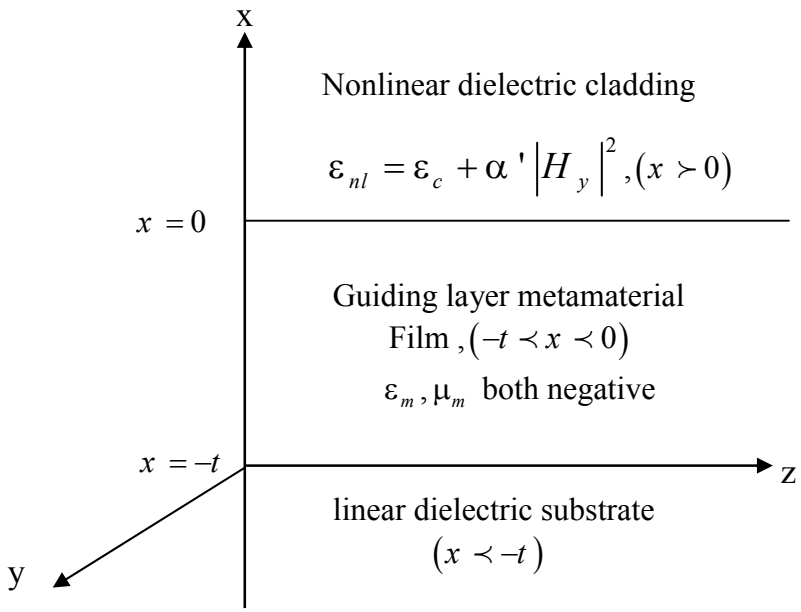

Fig.4.1 :The waveguide structure under consideration

The magnetic and electric fields of TM waves propagating in the z-direction are expressed as:

$$E = (E_x, 0, E_z) e^{j(\omega t - \beta z)} \tag{4-1}$$

$$H = (0, H_y, 0) e^{j(\omega t - \beta z)} \tag{4-2}$$

where $\beta = k_0 n_e$

For the case under consideration Eq. (1-47) can be written as :

$$\frac{\partial^2 H_y}{\partial x^2} + (\mu\varepsilon\omega^2 - \beta^2) H_y = 0 \tag{4-3}$$

We have confined our attention to p-polarized waves propagating in a thin film that exhibits no nonlinearity. The covering medium has an intensity-dependent dielectric constant ε_{nl} of Kerr-type $\varepsilon_{nl} = \varepsilon_c + \alpha |\mathbf{E}|^2$, where α is the nonlinear constant and ε_c is the linear part of the permittivity. To solve the nonlinear wave equation for the nonzero magnetic field component H_y, one can write ε_{nl} as [45,46] :

$$\varepsilon_{nl} = \varepsilon_c + \alpha' \left| H_y \right|^2 \qquad (4\text{-}4)$$

Where $\alpha' = \alpha / \varepsilon_c c^2 \varepsilon_o^2$, where c is the speed of light in vacuum, ε_0 is free space permittivity.

Equation (4-3) in the three layers takes the form :

$$\frac{\partial^2 H_{y_1}}{\partial x^2} - k_0^2 \left(n_e^2 - n_c^2 \right) H_{y_1} + \alpha_c' k_0^2 H_{y_1}^3 = 0, (x \succ 0) \quad \text{(cladding)} \qquad (4\text{-}5)$$

$$\frac{\partial^2 H_{y_2}}{\partial x^2} + k_0^2 (m n_f^2 - n_e^2) H_{y_2} = 0, \ (-t < x < 0) \qquad (\text{film}) \qquad (4\text{-}6)$$

$$\frac{\partial^2 H_{y_3}}{\partial x^2} - k_0^2 (n_e^2 - n_s^2) H_{y_3} = 0, \ (x < -t) \qquad \text{(substrate)} \qquad (4\text{-}7)$$

We recall the parameters q_c, q_s, and p given by:

$$q_c = \sqrt{n_e^2 - n_c^2}\ , \ q_s = \sqrt{n_e^2 - n_s^2}\ , p = \sqrt{m n_f^2 - n_e^2}$$

Exact solutions of Eqs. (4-5) to (4-7) are given by:

$$H_{y_1} = \sqrt{\frac{2}{\alpha'}} \frac{q_c}{\cosh\left[k_0 q_c \left(x + x_0 \right) \right]}, \ \left(x \succ 0 \right) \text{ (cladding)} \qquad (4\text{-}8)$$

$$H_{y_2} = B_m \cos(k_0 p x) + C_m \sin(k_0 p x), \ (-t < x < 0) \text{ (film)} \qquad (4\text{-}9)$$

$$H_{y_3} = D_m e^{k_0 q_s (x + t)}, \ (x < -t) \text{ (substrate)} \qquad (4\text{-}10)$$

The nonzero components of the electric field can be obtained using Eqs. (1-52), (1-53). They are given by:

$$E_{x_1} = \frac{k_0 n_e}{\varepsilon_0 \varepsilon_c \omega} \sqrt{\frac{2}{\alpha'}} \frac{q_c}{\cosh\left[k_0 q_c \left(x + x_0\right)\right]} \tag{4-11}$$

$$E_{x_2} = \frac{k_0 n_e}{\varepsilon_0 \varepsilon_f \omega} \left[B_m \cos(k_0 p x) + C_m \sin(k_0 p x)\right] \tag{4-12}$$

$$E_{x_3} = \frac{k_0 n_e}{\varepsilon_0 \varepsilon_s \omega} D_m e^{k_0 q_s (x+t)} \tag{4-13}$$

$$E_{z_1} = \frac{-k_0 q_c}{\varepsilon_0 \varepsilon_c j\omega} \sqrt{\frac{2}{\alpha'}} q_c \operatorname{sech}\left[k_0 q_c \left(x + x_0\right)\right] \tanh\left[k_0 q_c \left(x + x_0\right)\right] \tag{4-14}$$

$$E_{z_2} = \frac{k_0 p}{\varepsilon_0 \varepsilon_f j\omega} [-B_m \sin(k_0 p x) + C_m \cos(k_0 p x)] \tag{4-15}$$

$$E_{z_3} = \frac{k_0 q_s}{\varepsilon_0 \varepsilon_s j\omega} D_m e^{k_0 q_s (x+t)} \tag{4-16}$$

Matching the tangential components of **E** and **H** At $x = 0$, and $x = -t$, we get:

$$\sqrt{\frac{2}{\alpha'}} q_c \operatorname{sech} C = B_m \tag{4-17}$$

$$B_m \cos(k_0 p t) - C_m \sin(k_0 p t) = D_m \tag{4-18}$$

$$\frac{-k_0 q_c}{\varepsilon_0 \varepsilon_c j\omega} \sqrt{\frac{2}{\alpha'}} q_c \operatorname{sech} C \tanh C = \frac{k_0 p}{\varepsilon_0 \varepsilon_f j\omega} C_m \tag{4-19}$$

$$\frac{p}{\varepsilon_f} [B_m \sin(k_0 p t) + C_m \cos(k_0 p t)] = \frac{q_s}{\varepsilon_s} D_m \tag{4-20}$$

With some mathematical treatment of these relations, the following dispersion relation is obtained as :

$$k_0 p t = \tan^{-1}\left(\frac{x_s}{a_s}\right) + \tan^{-1}\left(\frac{x_c}{a_c} \tanh C\right) + N\pi \tag{4-21}$$

Where *N* is the number of modes.

4.2 Evaluation of the sensitivity

Differentiating the dispersion relation given by Eq. (4-21) with respect to n_e to obtain an expression for the sensitivity of the sensor. As a result we get:

$$S = \frac{\sqrt{a_c}\sqrt{1+x_c^2}\left[a_c H_m + a_c \tanh C + 2x_c^2 \tanh C\left(\frac{m-a_c}{1+x_c^2}\right)\right]}{x_c\sqrt{a_c+mx_c^2}\left(a_c^2+x_c^2\tanh^2 C\right)\left(T_m+T_{sm}+T_{cm}\right)} \tag{4-22}$$

Where:

$$H_m = k_0 x_0 x_c p\left(1-\tanh^2 C\right) \tag{4-23}$$

$$T_m = \tan^{-1}\left(\frac{x_s}{a_s}\right) + \tan^{-1}\left(\frac{x_c}{a_c}\tanh C\right) + N\pi \tag{4-24}$$

$$T_{sm} = \frac{a_s\left(1+x_s^2\right)}{x_s\left(a_s^2+x_s^2\right)} \tag{4-25}$$

$$T_{cm} = \frac{a_c H_m + a_c \tanh C\left(1+x_c^2\right)}{x_c\left(a_c^2+x_c^2\tanh^2 C\right)} \tag{4-26}$$

4.3 The condition of maximum sensitivity

Given a configuration of constant $\varepsilon_c, \varepsilon_f$ and ε_s, the condition of maximum sensitivity means what is the optimum thickness of the guiding layer at which the sensitivity of the proposed optical waveguide sensor has the highest value. This condition is achieved when the derivative of *S* with respect to *t* (the film width) vanishes [17,27,28] or $\frac{\partial S}{\partial t} = \frac{\partial S}{\partial x_s}\frac{\partial x_s}{\partial t} = 0$

Applying this methodology to Eq. (4-22) we get :

$$\sqrt{a_c}x_c\sqrt{a_c+mx_c^2}\theta d_1\left[\sqrt{1+x_c^2}j_2+\frac{j_1\omega x_s}{\sqrt{1+x_c^2}}\right]- \\ \sqrt{a_c}\sqrt{1+x_c^2}j_1\left[\sqrt{a_c+mx_c^2}x_c\theta\psi_4+d_1d_2\right]=0 \tag{4-27}$$

where

$$\beta=k_0x_0p\left[\omega\frac{x_s}{x_c}-\frac{x_sx_c}{1+x_s^2}\right] \tag{4-28}$$

$$\sigma=1-\tanh^2C\ , \qquad \theta=a_c^2+x_c^2\tanh^2C \tag{4-29}$$

$$\psi_1=\frac{a_c\left(x_c\sigma\beta+\tanh C\,\frac{\omega x_s}{x_c}\right)}{a_c^2+x_c^2\tanh^2C} \tag{4-30}$$

$$\psi_2=\frac{a_sx_s\left(a_s^2+x_s^2\right)\left(2x_s\right)-a_s\left(1+x_s^2\right)\left(a_s^2+3x_s^2\right)}{x_s^2\left(a_s^2+x_s^2\right)^2} \tag{4-31}$$

$$\psi_3=\frac{x_c\theta g_1-g_2g_3}{x_c^2\theta^2} \tag{4-32}$$

$$g_1=a_c\sigma_1+2a_c\tanh C\left(\omega x_s\right)+a_c\left(1+x_c^2\right)\sigma\beta \tag{4-33}$$

$$g_2=a_cH_m+a_c\tanh C\left(1+x_c^2\right) \tag{4-34}$$

$$g_3=a_c^2\omega\frac{x_s}{x_c}+2x_c^3\tanh C\left(\sigma\beta\right)+3\tanh^2C\left(\omega x_sx_c\right) \tag{4-35}$$

$$j_1=a_cH_m+a_c\tanh C+2\left(m-a_c\right)\tanh C\left(\frac{x_c^2}{1+x_c^2}\right) \tag{4-36}$$

$$j_2 =$$

$$a_c\sigma_1 + a_c\sigma\beta + 4\left(m - a_c\right)\tanh C\left[\frac{\omega x_s}{\left(1+x_c^2\right)^2}\right] + \left[\frac{2\left(m-a_c\right)x_c^2}{1+x_c^2}\right]\sigma\beta \qquad (4\text{-}37)$$

$$d_1 = T_m + T_{sm} + T_{cm} \qquad (4\text{-}38)$$

$$\psi_4 = \psi_1 + \psi_2 + \psi_3 \qquad (4\text{-}39)$$

$$d_2 = \sqrt{a_c + mx_c^2}\,g_3 + \frac{x_c\theta m\omega x_s}{\sqrt{a_c + mx_c^2}} \qquad (4\text{-}40)$$

4.4 Power flow within the layers for TM modes

For TM-waves, the energy flux per unit length is given by Eq. (1-59). Using Eqs. (4-8) to (4-10), the power flow through each layer can be obtained as follows :

$$P_c = \frac{n_e x_c p}{\omega\varepsilon_0\varepsilon_c\alpha'}\left[1 - \tanh C\right] \qquad (4\text{-}41)$$

$$P_f = \frac{n_e k_0}{2\omega\varepsilon_0\varepsilon_f}\left\{\frac{B_m^2}{2}x_- + \frac{C_m^2}{2}x_+ + \frac{B_m C_m}{k_0 p}\sin^2\left(k_0 pt\right)\right\} \qquad (4\text{-}42)$$

$$P_s = \frac{n_e D_m^2}{4\omega\varepsilon_0\varepsilon_s x_s p} \qquad (4\text{-}43)$$

Where :

$$B_m = \sqrt{\frac{2}{\alpha'}}q_c \operatorname{sec} hC \qquad (4\text{-}44)$$

$$C_m = \frac{-x_c^2 p}{a_c}\sqrt{\frac{2}{\alpha'}}\operatorname{sec} hC\,\tanh C \qquad (4\text{-}45)$$

and

$$D_m = \frac{a_s}{x_s}\left[B_m \sin(k_0 pt) + C_m \cos(k_0 pt)\right] \qquad (4\text{-}46)$$

The total power in the whole structure is given by:

$$P_{total} = \frac{n_e}{\omega\varepsilon_0}\left[\frac{x_c p}{\varepsilon_c \alpha'} y_1 + \frac{k_0}{2\varepsilon_f}\left\{\frac{B_m^2}{2} x_- + \frac{C_m^2}{2} x_+ + \frac{B_m C_m}{k_0 p}\sin^2(k_0 p t)\right\} + \frac{D_m^2}{4\varepsilon_s x_s p}\right] \quad (4\text{-}47)$$

The fraction of the total power flowing in the cladding is given by:

$$\frac{P_c}{P_{total}} = \frac{\frac{x_c p}{\varepsilon_c \alpha'} y_1}{\left[\frac{x_c p}{\varepsilon_c \alpha'} y_1 + \frac{k_0}{2\varepsilon_f}\left\{\frac{B_m^2}{2} x_- + \frac{C_m^2}{2} x_+ + \frac{B_m C_m}{k_0 p}\sin^2(k_0 p t)\right\} + \frac{D_m^2}{4\varepsilon_s x_s p}\right]} \quad (4\text{-}48)$$

4.5 Clad-Film interface nonlinearity

In chapter three, $\frac{\alpha E_o^2}{2}$ was defined as the clad-film interfacenonlinearity. In a similar manner we can define for TM modes $\frac{\alpha' H_o^2}{2}$ as clad-film interface nonlinearity, where H_0 represents the magnetic field at the clad-film interface (x = 0). In homogeneous sensing procedure, the material to be detected is uniformly distributed in the covering medium. As a result we will be concerned with clad-film interface nonlinearity. The magnetic field H_o is obtained by substituting x = 0 in Eq. (4-8), we get:

$$H_o = \sqrt{\frac{2}{\alpha'}}\,\frac{q_c}{\cosh C} \quad (4\text{-}49)$$

Equation (4-49) can be written as:

$$\frac{\alpha' H_o^2}{2} = q_c^2 (1 - \tanh^2 C) \quad (4\text{-}50)$$

One can substitute for tanh C from Eq. (4-50) into Eq. (4-22) to obtain an expression for the sensitivity of the proposed sensor as a function of the clad-film interface nonlinearity.

4.6 Results

The argument above offers a set of equations sufficient for determining all the parameters needed to design the sensor and bring it to its maximum sensing sensitivity. This can be achieved as follows:
given the asymmetry parameters a_c and a_s, one can substitute for x_c from Eq. (3-21) into the condition of maximum sensitivity given by Eq . (4-27) to end with a function of x_s only thus having the optimum value of x_s.

Substituting these values in the characteristic equation, we can compute the waveguide widths ensuring maximum sensitivity. The values of these maxima are calculated through substituting the last values in the expression of sensitivity. The surface $x_s\,(a_s,a_c)$ is shown in Fig. 4.2.

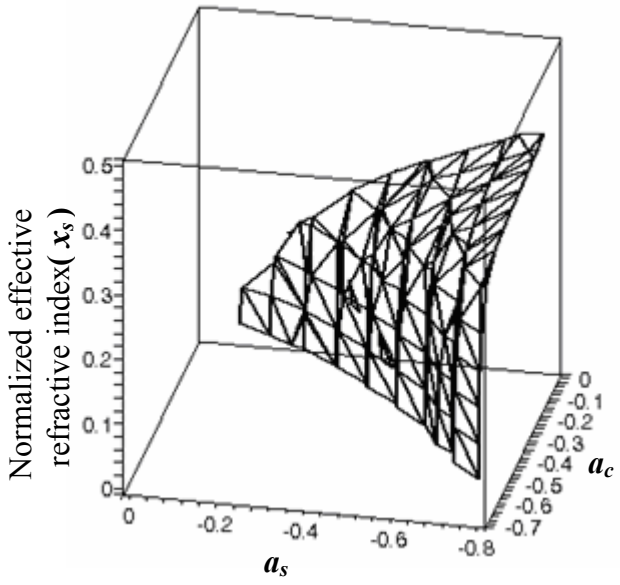

Figure 4.2. Normalized effective refractive index x_s versus a_s and a_c ensuring maximum sensitivity for homogeneous sensing.

Fig. 4.3 and Fig. 4.4 show the variation of the sensitivity of the proposed waveguide sensor with the asymmetry parameter a_c and with the asymmetry parameter a_s respectively. The sensitivity increases with increasing a_c and decreases with increasing a_s. This behavior is attributed to the power considerations. Increasing a_c and decreasing a_s enhance the power fraction flowing in the cladding medium which leads to enhancement of the optical sensitivity of the sensor.

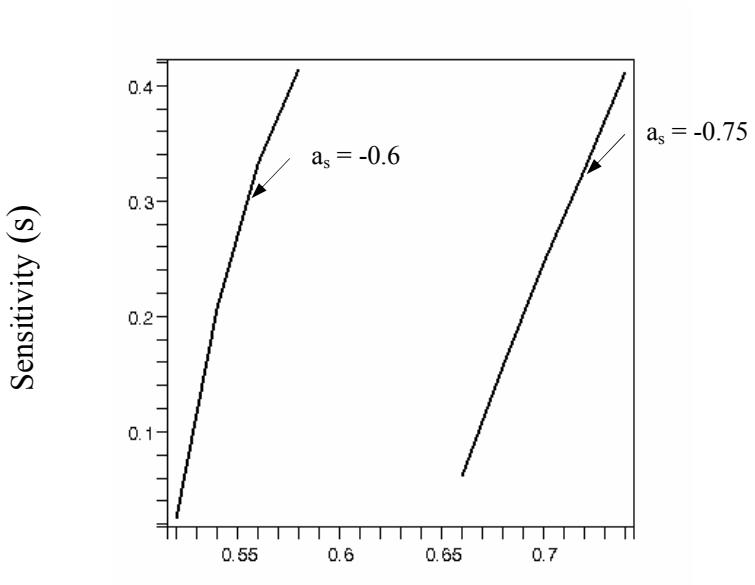

Figure 4.3. Sensitivity versus the absolute value of the asymmetry parameter a_c for the case of TM waves, for different values of a_s (-0.6, -0.75).

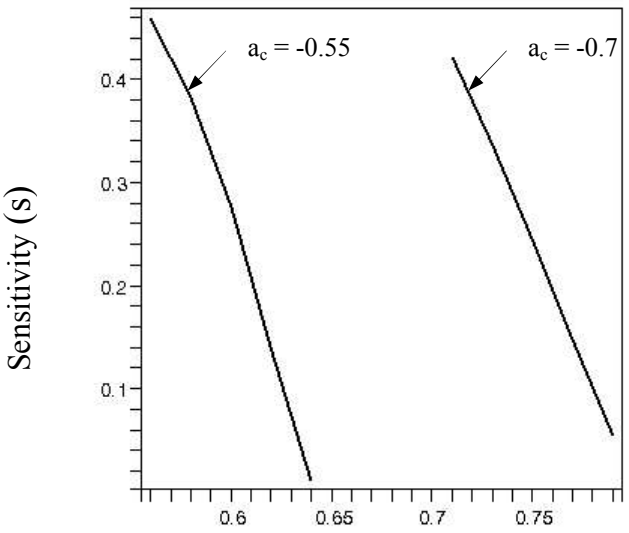

Figure 4.4. Sensitivity versus the absolute value of the asymmetry parameter a_s for the case of TM waves, for different values of a_c (-0.55, -0.7).

The variation of the sensitivity of the proposed sensor with $|m|$ is shown in Fig. 4.5. As can be seen, for small values of $|m|$ the sensitivity approaches zero due to the high confinement of the guided mode in the guiding layer. In the other limit, all the power of the mode propagates in the substrate. Consequently, the sensor probes the substrate side only and the sensitivity of the effective refractive index to variations in the index tends to zero. Between these two limits, there is a maximum in the sensitivity curves representing an optimum where a relatively large part of the total mode power propagates in the cladding.

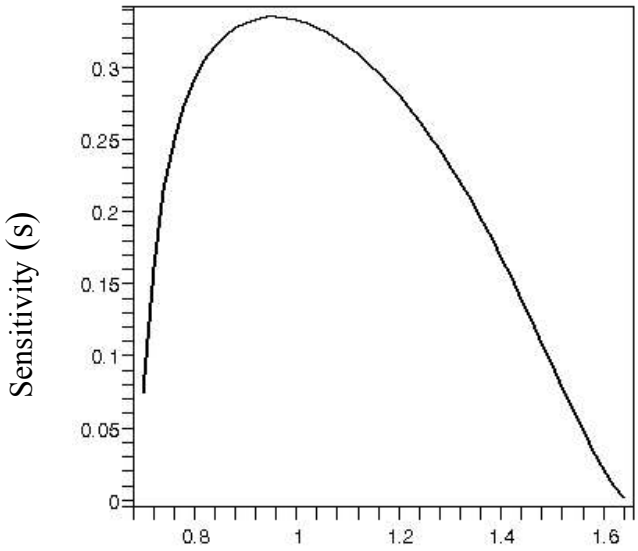

Figure 4.5. Sensitivity of the proposed sensor versus the absolute value of m where $\mu_m = m\mu_o$.

In Fig. 4.6 and Fig. 4.7 we study the variation of S with the nonlinear term arising from the nonlinearity of the cladding (tanhC) and with the fraction of power flowing in the cladding respectively.

As tanhC approaches one, the linear cladding case, the sensitivity goes to its minimum values. The relation between S and P_c/P_{total} is a straight line emphasizing the fact that the high degree of confinement in the guiding layer in the case of sensing applications is not recommended.

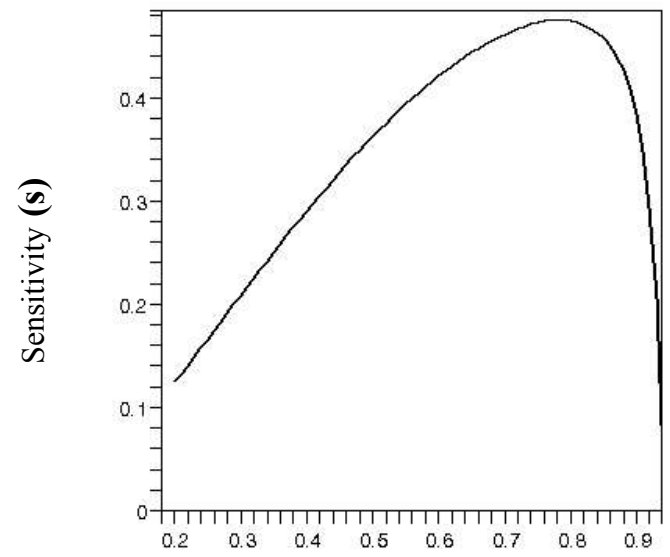

Figure 4.6. Sensitivity of the proposed optical waveguide sensor versus tanhC.

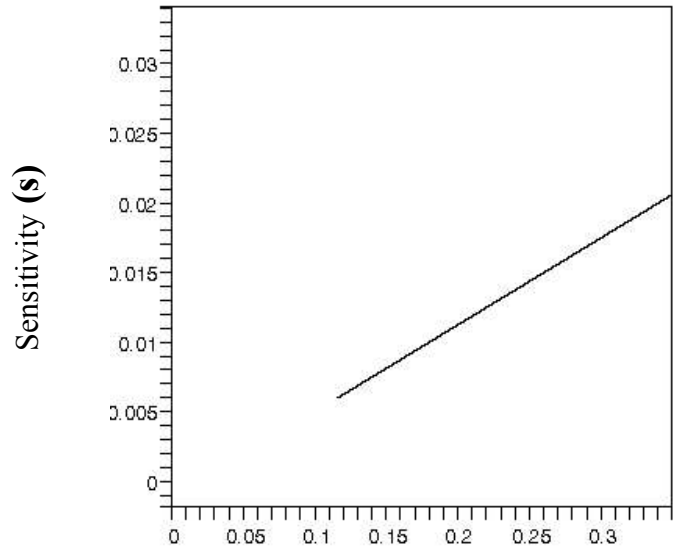

Figure 4.7. Sensitivity of the proposed optical waveguide sensor versus the fraction of total power flowing in the cladding.

The sensitivity of the proposed nonlinear sensor versus the clad-film interface nonlinearity $\frac{\alpha' H_o^2}{2}$ is shown in Fig. 4.8. The sensitivity increases with increasing the clad-film interface nonlinearity. As mentioned in chapter 3, as the clad-film interface nonlinearity increases the evanescent tail in the cladding increases and the sensitivity of the sensor is enhanced.

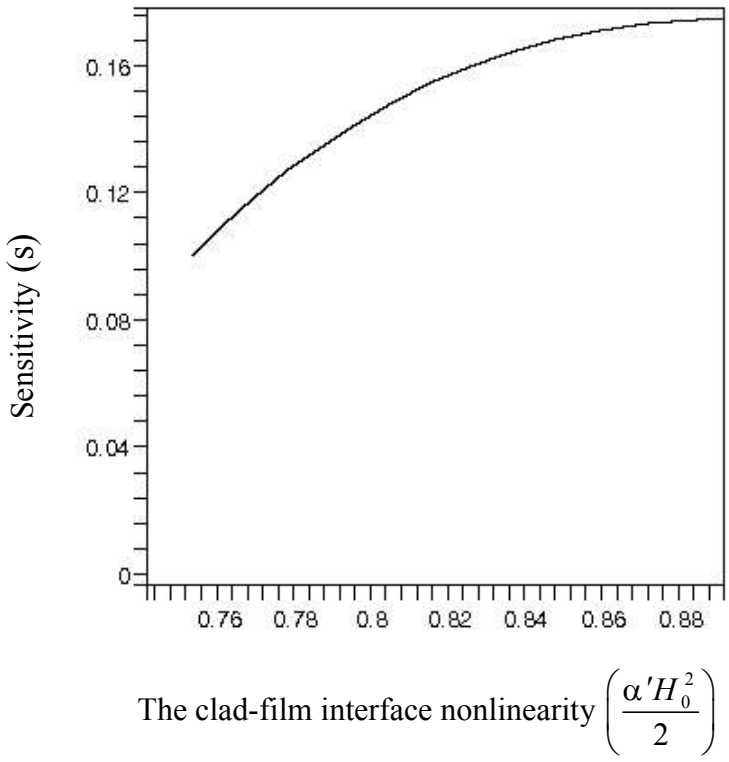

Figure 4.8 Sensitivity versus the clad-film interface nonlinearity

CHAPTER FIVE
CONCLUSION

The main purpose of this thesis was to propose new structures of optical waveguide sensors. We have presented comprehensive analytical studies on nonlinear optical waveguide sensors when the guiding layer is made of a Left-Handed material. A nonlinear cladding and a linear substrate were considered. Moreover, we investigated s-polarized waves (TE) and p-polarized waves (TM).

With respect to planar optical waveguide sensors, the main remarks gained from our investigations can be summarized as follows:

- There is a close connection between the fraction of total power propagating in the covering medium and the sensitivity of the sensor. In most cases, they may be regarded as nearly identical thus the enhancement of the fraction of total power flowing in the cladding is essential for sensing applications.

- As the nonlinearity of the cladding increases, the wave crest is displaced towards the cladding and as a result the sensitivity of the optical waveguide sensor is enhanced.

- The sensitivity increases with increasing the clad-film interface nonlinearity since increasing the nonlinear coefficient α will enhance the permittivity of the cladding. Hence the fraction of total power flowing in the cladding is enhanced. Moreover as the squared field magnitude at the clad-film interface increases the evanescent tail in the cladding increases and the sensitivity of the sensor also increases.

- Cladding to film permittivity ratio should be as high as possible but substrate to film permittivity ratio should be as low as possible to increase the evanescent field tail in the cladding and to reduce it as possible in the substrate. The inversion of the conventional waveguide symmetry is strongly recommended if possible. In some cases it is not possible especially when the analyte is air

- For small values of $|m|$ the sensitivity approaches zero due to the high confinement of the guided mode in the guiding layer. For high values all the power of the mode propagates in the substrate. Consequently, the sensor probes the substrate side only and the sensitivity of the effective refractive index to variations in the index tends to zero. Between these two limits, there is a maximum in the sensitivity curves representing an optimum where a relatively large part of the total mode power propagates in the cladding. The optimum value of μ for the Left-Handed Material is found to be near the free space permeability.

FUTURE WORK

The following thoughts are assumed to be put to research in the future:

- The study of nonlinear reverse asymmetry for it is reported that this configuration has promising properties. A sensor with a_c higher than a_s will be considered and the analysis carried out in this thesis will be shifted to this configuration.
- Analytical study of (all nonlinear) sensing pads, i.e. sensors with all layers being nonlinear special interest will be paid to the case of uniform field profile
- A more intensive point of view on the relation between power flowing in the sensor layers and its response will be set to test.
- An approach to more realistic metallic waveguide sensors will be set to research, a case when the current density J is considered.

REFERENCES

[1] K. Benaissa, A. Nathan, "Silicon anti-resonant reflecting optical waveguides for sensor applications", Sensors and Actuators A 65 (1998) 33-44

[2] R. G. C. Oudshoorn, R. P. H. Kooyman J. Greve, "Refractive index and layer thickness of an adsorbing protein as reporters of monolayer formation", Thin solid films 284-285 (1996) 836-840

[3] D. K. Qing, X. M. Chen, K. Itoh M. Murabayashi," A theoretical evaluation of the absorption coefficient of the optical waveguide chemical or biological sensors by group index method", J. of Lightwave Tech 14, 8 (1996) 1907-1917

[4] S. Plunkett, S. Propst M. Braiman," Supported planar germanium waveguides of infrared evanescent-wave sensing", App. Optics 36, 18 (1997) 4055-4061

[5] R. Bernini, S. Campopiano, and L. Zeni, "Design and analysis of an integrated antiresonant reflecting optical waveguide refractive index sensor", Appl. Opt., 41, 1, 70-73 (2002).

[6] D. K. Qing and I. Yamaguchi, "Analysis of the sensitivity of optical waveguide chemical sensors for TM modes by the group-index method", J. Opt. Soc. Am. B, 16, 9, 1359-1369 (1999).

[7] F. Prieto, A. Liobera, D. Jimenez, C. Domengues, A. Calla, and L. M. Lechuga, "Design and analysis of silicon antiresonant reflecting optical waveguide for evanescent field sensor", J. of Lightwave Tech., 18, 7, 966-972 (2000).

[8] N. Skivesen, R. Horvath, and H. Pedersen, "Multimode reverse-symmetry waveguide sensor for broad-range refractometry", Opt. Letters, 28, 24, 2473-2475 (2003).

[9] R. Horvath, L. R. Lindvold, and N. B. Larsen, "Fabrication of all polymer freestanding waveguides", 13, 419-424 (2003).

[10] K. Tiefenthaler and W. Lukosz, "Sensitivity of grating couplers as integrated-optical chemical sensors", J. Opt. Soc. Am. B, 6, 2, 209–220 (1989).

[11] L. Xu, J. C. Fanguy, Krunel Soni, and Shiquan Tao, "Optical fiber humidity sensor based on evanescent-wave scattering", Optics Lett., 29, 11, 1191-1193 (2004).

[12] K. A. Remley and A. Weisshaar, "Design and analysis of a silicon-based antiresonant reflecting optical waveguide chemical sensors ", Optics Lett., 21, 16, 1241-1243 (1996).

[13] W. Lukosz, "Integrated optical chemical and direct biochemical sensors", Sensors and Actuators B, 29, 37-50 (1995).

[14] R. E. Kunz, "Miniature integrated optical modules for chemical and biochemical sensing", Sensors and Actuators B, 38, 13-28 (1997).

[15] R. Horvath, H. C. Pederson, and N. B. Larsen, "Demonstration of reverse symmetry waveguide sensing in aqueous solutions", App. Phys. Lett., 81, 12, 2166-2168 (2002).

[16] O. Parriaux and P. Dierauer, "Normalized expressions for the optical sensitivity of evanescent wave sensors", Opt. Lett., 19, 7, 508-510 (1994).

[17] O. Parriaux and G. J. Velduis, "Normailzed analysis for the sensitivity optimization of integrated optics evanescent-wave sensors", J. of Light Tech., 16, 4, 573-582 (1998).

[18] G. J. Veldhuis, O. Parriaux, H. J. W. M. Hoekstra, and P. V. Lambeck, "Sensitivity enhancement in evanescent optical waveguide sensor", J. of Lightwave Tech., 18, 5, 667-682 (2000).

[19] O. Parriaux, P. V. Lambeck, H. J. W. M. Hoekstra, G. J. Veldhuis, and G. Pandraud, "Evanescent wave sensor of sensitivity larger than a free space wave", Opt. and Quantum Electronics, 32, 909-921 (2000).

[20] G. J. Veldhuis, O. Parriaux, and P. V. Lambeck, "Normalized analysis for the optimization of geometric wavelength dispersion in three-layer slab waveguides" Opt. Comunication, 163, 278-284 (1999).

[21] A. Schilling, O.Yavas, J. Bischof, J. Boneberg, and P. Leiderer, "Absolute

preasure measurement on nanosecond scale using surface plasmons", Appl. Phys. Lett., 69, 27, 4159-4161 (1996).

[22] J. Ctyroky, J. Homola, and M. Skalsky, "Modeling of surface plasmon resonance waveguide sensor by complex mode expansion and propagation method", Opt. and Quant. Elect., 29, 301-311 (1997).

[23] J. Ctyroky, J. Homola, P. V. Lambeck, S. Musa, H. J. Hoekstra, R. D. Harris, J. S. Wilkinson, B. Usievich, and N. M. Lyndin, "Theory and modeling of optical waveguide sensors utilizing surface plasmon resonance", Sensors and Actuators B, 54, 66-73 (1999).

[24] R. Bernini, S. Campopiano, L. Zeni, "Leakage Properties of ARROW Waveguides for Chemical and Biochemical Sensing Applications", Proc. SPIE, Photonic Boston '01, 4578. (2001).

[25] R. Bernini, S. Campopiano, and L. Zeni, "Design and analysis of an integrated antiresonant reflecting optical waveguide refractive index sensor", Appl. Opt., 41, 1, 70-73 (2002).

[26] M.M. Shabat, H. Khalil, S. A. Taya, and M.M. Abadla, "Analysis of the sensitivity of self-focused nonlinear optical evanescent waveguide sensors", International Journal of Optomechatronics, 1, 284-296 (2007).

[27] H.M. Khalil, M.M. Shabat, S. A. Taya, and M.M.Abadla, "Nonlinear optical waveguide structure for sensor application: TM case", Int. J. of Modern Phys. B, 21, 30, 5075-5089 (2007).

[28] S. Taya, M. M. Shabat, and M. M.Abadla, and H. M. Khalil, " Analysis of the sensitivity of Integrated Nonlinear Optical Evanescent wave sensors", Proc. of SPIE Vol. 6585, 65851A-1-9, (2007)

[29] D. Griffiths, Introduction to electrodynamics, Prentice Hall, 3rd edition, (1999).

[30] R. Dubroff, S. Marshal, and G. Skitek, Electromagnetic concepts and applications, Prentice Hall, 4th edition, (1996).

[31] A. H. Cherin, An introduction to optical fibers, McGraw-Hill Book Company, 1st edition, (1993).

[32] C. P. Pollock, Fundamentals of optoelectronics, Richard D. Irwin Inc, (1995)

[33] M. N. O. Sadiku, Elements of Electromagnetism, Oxford University Press, 3rd edition, (2001).

[34] P. Lorrain and D. Corson, Electromagnetic fields and waves, W. H. Freeman and Company, 2nd edition, (1970)

[35] C. L. Chen, Elements of optoelectronics and fiber optics, Irwin, (1996).

[36] V. G. Veselago, "The electrodynamics of substance with simultaneously negative values of ε and μ", Sov. Phy.Usp., 10, 4, 509-514 (1968).

[37] R. Shelby, D. Smith, and S. Schultz, "Experimental verification of a negative index of refraction", Science, 292,5514, 77-79,(2001).

[38] J. B. Pendry, "Negative refraction makes a perfect lens", Phys. Rev Lett., 85, 18, 3966-3969 (2000).

[39] A. Gribc and G. Eleftheriades, "Growing evanescent waves in negative-refractive index", App. Phys. Lett., 82, 12, 1815-1817 (2003).

[40] A. Ankiewics and H. T. Tran, "A new class of nonlinear guided waves", J. of modern opt., 38, 6, 1093-1106 (1991).

[41] C. Seaton, J. Valera, R. Shoemaker and others, "Calculations of nonlinear TE waves guided by thin dielectric films bounded by nonlinear media", IEEE J. of Quantum Elec., QE 21, 7, 774-782 (1985).

[42] L. Wu, S.She, J. Wang, and L. Fan, "Amplitude-identical core field of TE_o modes in three-layer slab waveguides with nonlinear claddings", Opt. Comm., 185, 221-225 (2000).

[43] C. Xuelong, H. Zhaoming, and Z. Yowei, "Spatial bistability in nonlinear optical waveguides ", Chinese Phys.-Lasers, 15, 5, 381-383 (1988).

[44] R. Horvath, L. R. Lindvold and N. B. Larsen, "Reverse-symmetry waveguides: theory and fabrication", App. Phys. B, 74, 383-393 (2002).

[45] D. Mihalache, R. G. Nazmitdinov, and V. K. Fedyanin, "Nonlinear optical waves in layered structures", Sov. J. Part. Nucl., 20, 1 (1989) 86-107.

[46] George I. Stegeman and Colin T. Seaton, "Nonlinear surface plasmons guided by thin metal films", Opt. Lett., 9, 6 (1984) 235-237.